Miner Deposita (2006) 41: 671–690
DOI 10.1007/s00126-006-0079-1

ARTICLE

Paul Macey · Chris Harris

Stable isotope and fluid inclusion evidence for the origin of the Brandberg West area Sn–W vein deposits, NW Namibia

Received: 3 June 2005 / Accepted: 15 June 2006 / Published online: 24 August 2006

Abstract The Brandberg West region of NW Namibia is dominated by poly-deformed turbidites and carbonate rocks of the Neoproterozoic Damara Supergoup, which have been regionally metamorphosed to greenschist facies and thermally metamorphosed up to mid-amphibolite facies by Neoproterozoic granite plutons. The meta-sedimentary rocks host Damaran-age hydrothermal quartz vein-hosted Sn–W mineralization at Brandberg West and numerous nearby smaller deposits. Fluid inclusion microthermometric studies of the vein quartz suggests that the ore-forming fluids at the Brandberg West mine were CO_2-bearing aqueous fluids represented by the NaCl–$CaCl_2$–H_2O–CO_2 system with moderate salinity (mean=8.6 wt% $NaCl_{equivalent}$). Temperatures determined using oxygen isotope thermometry are 415–521°C (quartz–muscovite), 392–447°C (quartz–cassiterite), and 444–490°C (quartz–hematite). At Brandberg West, the oxygen isotope ratios of quartz veins and siliciclastic host rocks in the mineralized area are lower than those in the rocks and veins of the surrounding areas suggesting that pervasive fluid–rock interaction occurred during mineralization. The O- and H-isotope data of quartz–muscovite veins and fluid inclusions indicate that the ore fluids were dominantly of magmatic origin, implying that mineralization occurred above a shallow granite pluton. Simple mass balance calculations suggest water/rock ratios of 1.88 (closed system) and 1.01 (open system). The CO_2 component of the fluid inclusions had similar $\delta^{13}C$ to the carbonate rocks intercalated with the turbidites. It is most likely that mineralization at Brandberg West was caused by a combination of an impermeable marble barrier and interaction of the fluids with the marble. The minor deposits in the area have quartz veins with higher $\delta^{18}O$ values, which is consistent with these deposits being similar geological environments exposed at higher erosion levels.

Keywords Brandberg West · Tin–tungsten · Stable isotopes · Fluid inclusions · Namibia

Editorial handling: C. Marignac

P. Macey · C. Harris (✉)
Department of Geological Sciences, University of Cape Town,
Rondebosch, 7700, South Africa
e-mail: charris@geology.uct.ac.za
Tel.: +27-21-6502921
Fax: +27-21-6503783

Present address:
P. Macey
Council for Geoscience,
P.O. Box 572 Bellville, 7535, South Africa

Introduction

Most authors (e.g., Burnham 1997; Roedder 1984; Pirajno 1992) agree that hydrothermal Sn–W deposits are generally associated with granite magmatism. There is less agreement as to the mechanism of Sn and W concentration and the mechanism of precipitation of Sn–W from the ore-forming fluid. Explanations for the former include crystal/melt fractionation processes and partial melting of a metal-rich sedimentary source, whereas explanations for the latter include mixing with meteoric water, interaction with the country rocks, and fluid immiscibility. In this study, a combination of new fluid inclusion and stable isotope data, with field observations, and existing petrological data is used to constrain the chemistry of the mineralizing fluids, to determine the temperature and pressure conditions of mineralization and the probable source of mineralizing fluids in the Brandberg West and related Sn–W deposits. In addition, it was possible to test the cassiterite oxygen isotope fractionation factors recently published by Polyakov et al. (2005) and Hu et al. (2005).

The Sn–W deposits of Damaraland, NW Namibia, were subdivided into four NE-trending belts, which occur in the southern Kaoko zone and the central and northern zones of the Damara Province (Pirajno and Jacob 1987b; Diehl 1992a,b; Miller 1992). From south to north, the belts are known as the Erongo–Karibib belt, Neneis–Kohero belt, Strathmore–Uis belt, and the Brandberg West–Goantagab belts. The Erongo–Karibib belt consists of Sn ± Ta ± W pegmatites and W-bearing greisen deposits. The central group, comprising the Neneis–Kohero and Strathmore–

Uis belts, contains Sn–Ta pegmatites associated with syn- to post-tectonic granites (Pirajno and Jacob 1987b; Miller 1992).

The Brandberg West area, situated in the northernmost tin belt (Fig. 1), is dominated by the tightly folded Zerrissene Group turbidites and minor carbonate rocks, which form part of the Neoproterozoic Damara Supergroup. Most of the Sn (± Ag ± base metals) and Sn–W deposits of the Brandberg West area are hosted in hydrothermal veins and iron-rich replacement bodies; however, Sn–Ta bearing pegmatites also occur. The main deposits in the area are the Brandberg West mine (Sn–W hydrothermal vein-type) and the Frans (Sn hydrothermal vein-type), Gamigab (Sn hydrothermal vein-type), and Goantagab (hydrothermal vein- and replacement-type Sn) prospects. The hydrothermal vein and replacement-type deposits and the related thermal metamorphism and hydrofracturing clearly postdate the regional Neoproterozoic Damara fabrics, but the actual age of the deposits has been somewhat controversial. The mineralization has been

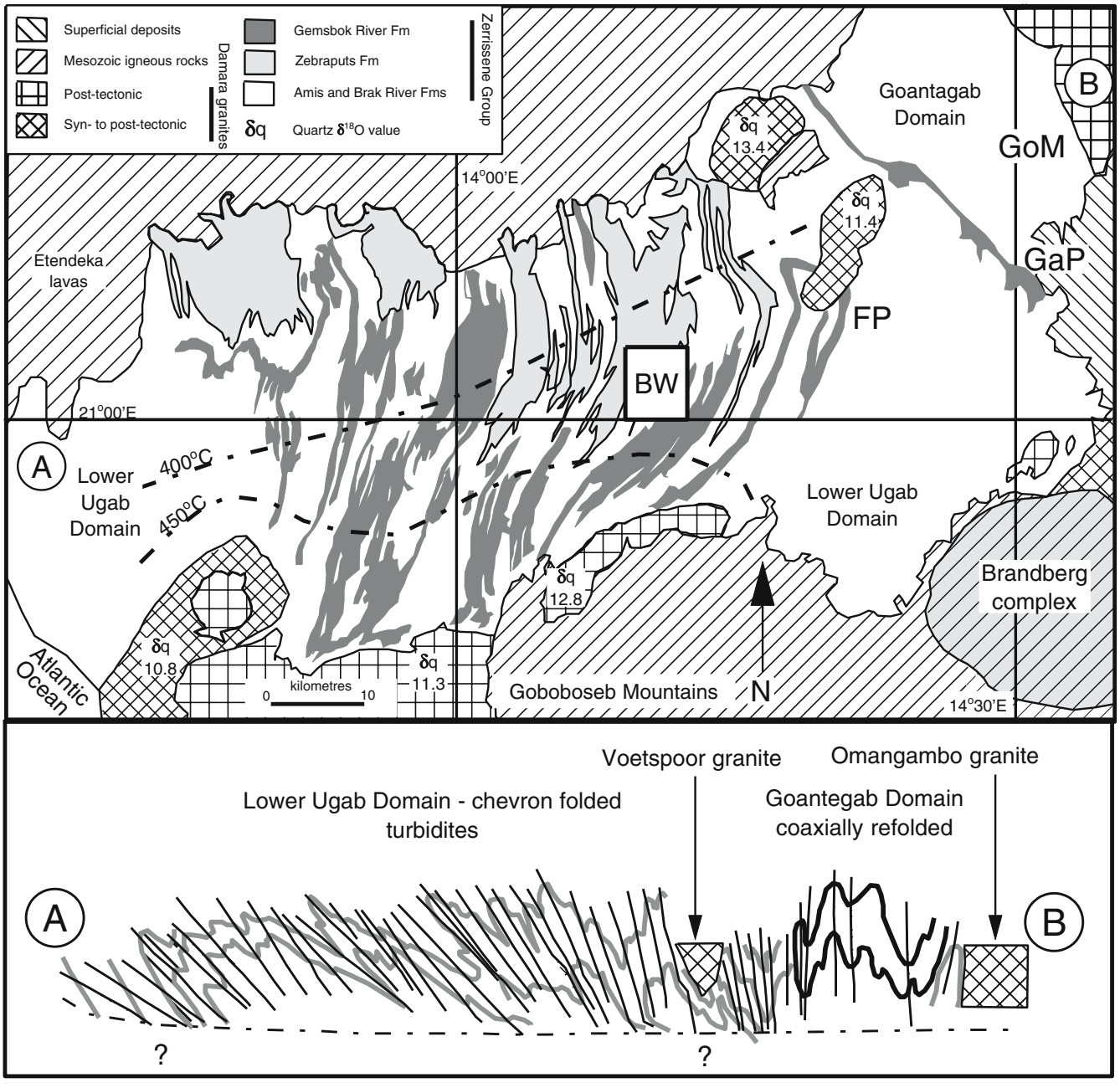

Fig. 1 Summary geological map of Brandberg West area based on Freyer (unpublished) with a schematic cross section summarized from Goscombe et al. (2004). The Lower Ugab domain is the large area N and S of Ugab River. The Goantagab Domain is smaller area in the NE. *GoM* Goantagab mineralized area, *GaP* Gamigab prospect, *FP* Frans prospect, *BW* Brandberg West mine area. The *rectangle* indicates the area shown in Fig. 2. The 400 and 450°C metamorphic contours are from Goscombe et al. (2004). The Brandberg Complex is Mesozoic in age and is part of the Etendeka Igneous Province. Quartz $\delta^{18}O$ values given for the granites are from Macey (2003)

considered to be linked to either the post-tectonic Damara granitoid magmatic activity (e.g., Miller 1983, 1992; Diehl 1992a,b; Pirajno et al. 1992/93; Jacob and Kruger 1994), or to granitic varieties of the Mesozoic anorogenic alkaline complexes (Pirajno and Jacob 1987a,b; Wagener 1989). However, Rb–Sr dating of the Goantagab, Gamigab (509±11 Ma), and Brandberg West vein systems indicates that mineralization was coeval with Damaran magmatism (Walraven 1989; Jacob and Kruger 1994).

Although the general geological settings and characteristics of the main Sn–W deposits in the Brandberg West area have been relatively well-researched and well-documented (Bentley 1985; Elliot 1985; Osborn 1985; Maclaren 1993; Townshend 1985; Petzel 1986; Pirajno and Jacob 1987a,b; Pirajno et al. 1987; Walraven 1988,1989; Bowen 1984; Potgieter 1984; Vickers 1984; Bowen and Evers 1989), no O, H, and C isotope studies were performed and only preliminary fluid inclusion studies were carried out. This study aims to use fluid inclusions and stable isotope geochemistry, in conjunction with field observations, (1) to constrain the chemistry of the mineralizing fluids, (2) to determine the temperature and pressure conditions of mineralization, and (3) to suggest the probable source of mineralizing fluids. This study concentrates on the Brandberg West mine and only preliminary isotope and microthermometric results from the Frans and Goantagab deposits are presented. The study forms part of an extensive regional stable isotope and fluid study (Macey 2003).

Regional geology

The Brandberg West area is divided into the Lower Ugab and the Goantagab tectonostratigraphic domains (Hoffmann 1987; Hoffman et al. 1996; Fig. 1). The Lower Ugab Domain covers the central parts of the Brandberg West area and it consists entirely of the tightly folded, siliciclastic turbidites (88%) and carbonate rocks (12%) of the Zerrissene Group of the Damara Supergroup (Swart 1987). The 1,700-m thick succession is subdivided into five conformable and laterally persistent lithostratigraphic units. The three siliciclastic units, the Zebrapüts, Brak River, and Amis River Formations, are interbedded with two thin mixed carbonate–siliciclastic units, the Brandberg West and Gemsbok River Formations (Swart 1987; Milner 1997). The Zerrissene Group have been regionally metamorphosed to greenschist facies and thermally metamorphosed up to mid-amphibolite facies by intrusive granite plutons.

The Goantagab Domain is situated in the northeastern parts of the Brandberg West area (Fig. 1) and consists of upper greenschist facies pelitic schists and marbles of the Swakop Group of the Damara Supergroup (Osborn 1985; Maclaren 1993). The pelitic schists of the Orusewa Formation form the basal unit and are overlain by tillites and conglomerates of the Chuos Formation. The overlying Karibib Formation consists of two marble units separated by pelitic schist. The Kuiseb Formation quartzites form the uppermost part of the succession. The fact that both the Lower Ugab and Goantagab Domains consist of three meta-pelitic units separated by two carbonate horizons has led Petzel (1986) to suggest that the stratigraphy of these domains may be correlated.

The rocks of the Brandberg West area (Fig. 1) were folded during two Neoproterozoic Pan-African deformation events, D_1 and D_2 (Hälbich and Freyer 1985; Hoffman et al. 1996). In the Lower Ugab Domain, the D_1-event is characterized by spectacular NNE-trending tight F_1 folds, with moderate to steeply inclined east-dipping fold axial planes, near-horizontal fold axes, and a well-developed slaty cleavage. These folds are interpreted to be the result of the east–west compression associated with the closure of the Proto-Atlantic Ocean (Hälbich and Freyer 1985; Hoffman et al. 1996). The deformation was accompanied by the intrusion of numerous and voluminous syn- to post-tectonic Pan-African granitoid bodies (ca. 590–530 Ma; Seth et al. 1998; Jung et al. 2000, 2003; Goscombe et al. 2004), and wide (up to 15 km) thermal aureoles have developed adjacent to the main intrusive bodies (Fig. 1). The Damaran granites in general are dominated by S-type granites (Miller 1983; Jung et al. 2000, 2003), and the Damaran granites within the area of Fig. 1 have quartz $\delta^{18}O$ values ranging from 10.8 to 14.8‰, which suggest that they are of S-type affinity (Macey 2003).

Microfabric studies (Macey 2003; Goscombe et al. 2004) suggest that the heat provided by the intrusive rocks collectively added to the regional thermal budget and thus have been a primary cause of regional metamorphism (Macey 2003). Thermal metamorphism appears to have at least partly driven regional metamorphism because regional metamorphic isograds (Fig. 1) are roughly parallel to the granite contacts and the lowest grades of regional metamorphism are found in rocks the farthest away from the main granite intrusions. Thus, the area shown in Fig. 1 can be divided into a northwestern part where the metamorphism is regional and dominated by chlorite–muscovite schists. With increasing grade to the south and east, the muscovite is replaced by biotite–muscovite schists, biotite–andalusite schists, and close to the contacts with granites, cordierite–andalusite hornfelses. Similarly, mineralogical changes in the marly carbonate rocks grade from the muscovite to phlogopite, actinolite, zoisite, and diopside zones toward the granite contacts. When the petrographic results and petrological factors are taken into consideration, the peak thermal conditions (combined regional and contact metamorphism) are estimated to vary as a continuum between approximately 350°C in the chlorite/muscovite zone to 550–600°C at the granite contacts. In addition, pressures are estimated to be between 1.5 and 3.2 kbar (Macey 2003). Goscombe et al. (2004) gave estimates of pressure associated with contact metamorphism in the region of Brandberg West of 3.2± 1.0 kbar.

North and south of the Brandberg West area, the metaturbidites and granitoids are unconformably overlain by the undeformed Jurassic and Cretaceous Karoo Supergroup sedimentary rocks and Etendeka Group volcanic rocks (Fig. 1; Milner 1997). The 25-km diameter Mesozoic

Brandberg Complex is situated at the southeastern margin of the Lower Ugab Domain and consists mainly of alkaline granite (Diehl 1990).

Brandberg West deposit

The Brandberg West mine is located in the central parts of the Lower Ugab Domain (Figs. 1 and 2) and represents the largest known Sn–W deposit in the study area. Mining at Brandberg West commenced in early 1946 with alluvial workings followed by shallow underground mining (Evers and Bowen 1989). In 1957, the mine became open cast and the operation continued until closure in 1980. Fourteen thousand three hundred seventy-four tons of concentrate was recovered at grades of 32–56% tin oxide and 14.5–19% tungsten oxide (Diehl 1992a). The anastomosing sheet-like quartz vein system extends for at least 4 km in a northeasterly direction (Fig. 2), but the principal ore deposits are restricted to an area of 900×300 m. The network of mineralized veins is hosted predominantly within the core of a large F_1 anticline (Fig. 2) cross-cutting the quartz–biotite phyllites of the Zebrapüts Formation, but terminating against the overlying folded cap of carbonate rocks of the Brandberg West Formation (Fig. 2; Jeppe 1952; Bowen and Evers 1989).

Townshend (1985) identified three main quartz vein generations in the Brandberg West mine:

1. Early syn-orogenic veins
   The oldest veins, here referred to as the "early veins," consist almost entirely of quartz (minor muscovite, fluorite, and tourmaline) and are not associated with cassiterite or wolframite mineralization or wall rock metasomatism. These deformed early veins are probably representatives of the regional syn-metamorphic veins and predate the mineralization episode. Syn-orogenic veins are ubiquitous across the Brandberg West area (Figs. 1 and 2) and are generally monomineralic, with quartz being the principal infilling mineral, although calcite is not uncommon.
2. Greisen-type veins
   The veins associated with the Sn–W mineralization have typical greisen-type mineral compositions and morphological characteristics (Pirajno 1992). The ore-bearing veins are usually bounded by a muscovite selvage and contain, in addition to quartz (70–95%), variable amounts of cassiterite, wolframite, scheelite, fluorite, tourmaline, beryl, graphite, hematite, and sulfides. The anastomosing networks of sheetlike veins

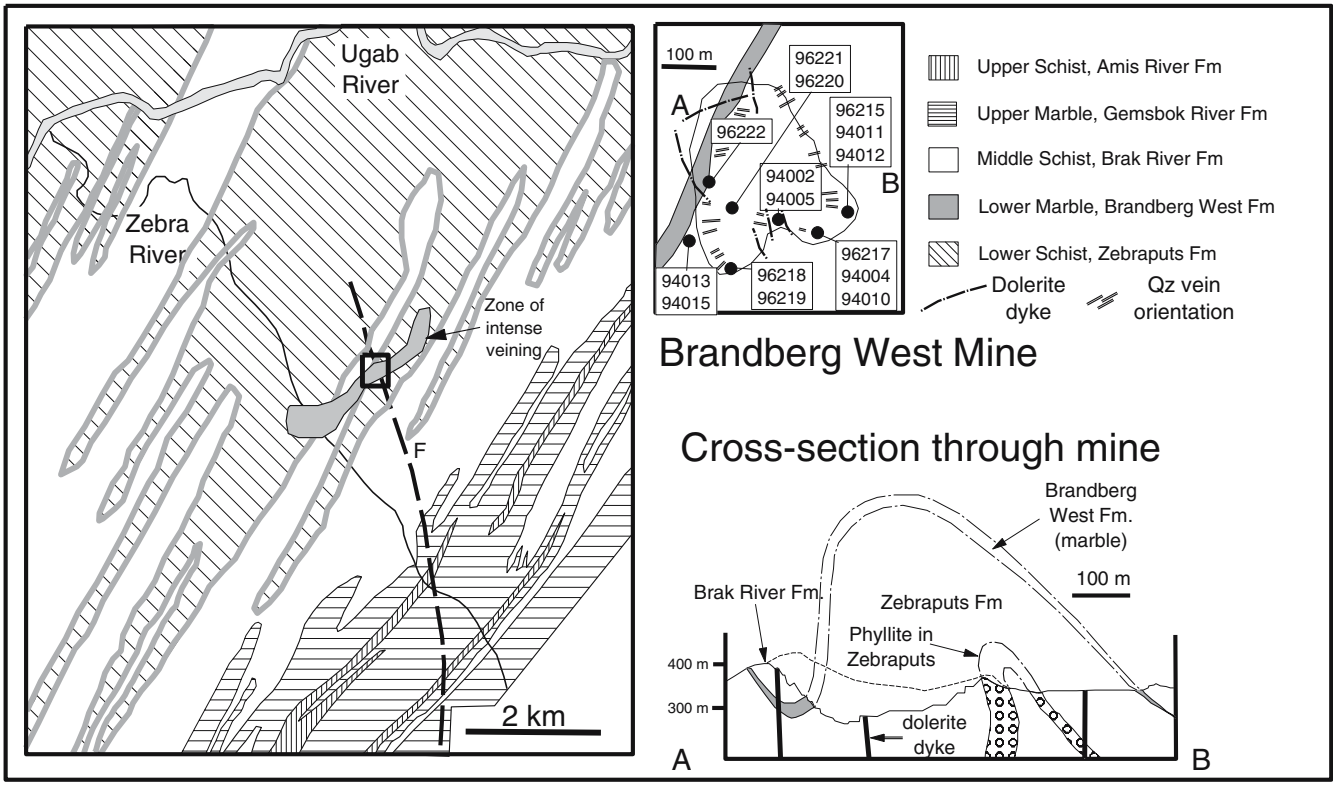

Fig. 2 Map of Brandberg West mine area (main figur e) showing location of zone of intense veining. *Upper right figure* shows pit outline and location of samples and location of dolerite dykes and orientation of quartz veins. Map modified from Petzel (1986). *Lower right* figure is a schematic cross section through Brandberg West deposit showing the outline of the open cast pit, looking NNE (adapted from Townshend 1985 and Petzel 1986)

crosscut the regional fabric and clearly postdate the regional deformation. The wall rocks adjacent to the fracture-controlled greisen veins were metasomatized during vein formation and a distinctive sequence of alteration minerals developed. The rocks directly adjacent to the greisen selvage were pervasively tourmalinized, and this tourmaline-rich zone grades into a muscovite–quartz zone followed by a zone of country rock sericitization (Elliot 1985). An early greisen stage produced a quartz–muscovite–cassiterite–wolframite assemblage, followed by distinct, but probably temporally overlapping phases, of quartz–sericite–cassiterite–fluorite–tourmaline and cassiterite–hematite–graphite–sulfide mineralization (Townshend 1985; Pirajno and Jacob 1987a,b).

3. Carbonate alteration, associated with hematite-bearing quartz veins and quartz–calcite veinlets, which crosscut all of the other veins, represent the final stages of hydrothermal activity (Townshend 1985; Pirajno 1992).

The biotite phyllites and marls and the phlogopite marbles hosting the hydrothermal Sn–W vein deposits of the Brandberg West mine were thermally metamorphosed during the formation of the deposits. The siliciclastic rocks were overprinted by biotite hornfels, and the marls of the Brandberg West Formation have biotite–orthoclase–cordierite–actinolite–diopside–zoisite and calcite–quartz–diopside assemblages (Jeppe 1952). Marly quartzites containing post-tectonic radiating aggregates of actinolite were also observed (Bowen and Evers 1989). In addition to the thermal metamorphism, various parts of the mineralized area are associated with broadscale pervasive Fe (hematite), K (sericite/muscovite), carbonate wall rock alteration, and tourmalinization (Jeppe 1952; Elliot 1985).

Minor Sn–W deposits

The Sn–W deposits of the Frans prospect (Petzel 1986) are situated within the eastern limb of a tight F_1 fold near the contact between the Brak River and Gemsbok River Formations in the central northeastern parts of the Lower Ugab Domain (Fig. 1). The stockwork of N, NNE, and NE-trending quartz veins can be followed for 3 km along a NNE-trending zone, but the Sn–W mineralization is concentrated in the area of highest vein density (Potgieter 1984). The veins consist predominantly of quartz with minor amounts of cassiterite, tourmaline, muscovite, iron oxides, sulfides (pyrite and chalcopyrite), and secondary malachite and chrysocolla (Potgieter 1984; Pirajno and Jacob 1987b). The cassiterite and wolframite occur sporadically in vugs and fractures in the quartz veins (Petzel 1986), and wall rock alteration is not as prominent as at the Brandberg West mine.

The Sn ± Ag ± Zn and sulfide deposits of the Goantagab mining district are located in the Goantagab domain approximately 30 km northeast of the Brandberg West mine and represent the northernmost example of cassiterite mineralization in the Brandberg West area (Fig. 1). The mineralization is hosted in the intercalated tremolite marbles and biotite–muscovite phyllites of the Karibib Formation and occurs as iron-rich, cassiterite-bearing replacement bodies in the marble and as cassiterite–sulfide–bearing quartz veins in the phyllites (Pirajno and Jacob 1987b). The surrounding country rocks are pervasively altered with tourmalinization and silicification having occurred adjacent to the veins, followed outwards by sericitization (Pirajno and Jacob 1987b).

The Gamigab deposit is located along the southeastern margin of the Goantagab Domain (Fig. 1). The Sn mineralization is hosted in E–W trending quartz veins, which crosscut the quartz–biotite phyllites of the Orusewa Formation (Pirajno and Jacob 1987a; Walraven 1988). The deposit is situated within an antiformal structure (F_1-equivalent), and the mineralization is capped by the Karibib Formation marbles, which appear to have acted as a chemical and/or physical barrier to the fluids (Walraven 1989).

Analytical procedures

Fluid inclusion microthermometric studies were carried out on a FLUID INC.-adapted USGS N_2 gas flow heating–freezing stage, housed in the Department of Geological Sciences at the University of Cape Town. The microthermometric equipment was calibrated using H_2O (0.75 mol%)–CO_2 (0.25 mol%) and pure H_2O SYNFLINC synthetic fluid inclusion standards (distributed by FLUID INC.; Sterner and Bodnar 1984). With the use of these standards, the system was calibrated against the triple point of CO_2 (−56.6°C), the triple point of water (0.0°C), and the critical point of water (374±1°C). Accuracy is estimated to be better than ±0.2°C below 0 and ±1°C on heating the sample (Frimmel et al. 1999). In an attempt to avoid the effects of post-entrapment modifications such as leaking and necking down, only those fluid inclusion clusters or trails with consistent volumetric liquid to vapor ratios were selected. Samples containing aqueous two-phase ($L_{aq} + V_{aq}$) inclusions were cooled to below −70°C, and the temperatures of the following phase changes were recorded on heating: first melting (T_e), final melting (T_m), and total homogenization (T_h). Given the low salinities of the inclusions, T_e observations were often relatively difficult to make. The carbonic three-phase ($L_{aq} + L_{carb} + V_{carb}$) inclusions were cooled until freezing of the carbonic component at about −95 to −100°C (clearly visible as the inclusion "splinters"). The following phase changes were observed during heating: CO_2 final melting, final melting of gas hydrate, CO_2 homogenization, and total homogenization (rarely achieved since the inclusions often decrepitated before total homogenization). The carbonic two-phase ($L_{carb} + V_{carb}$) fluid inclusions were cooled as the carbonic three-phase inclusions, and the temperatures of the CO_2-triple point and the CO_2 homogenization were recorded.

All stable isotope measurements were made at the University of Cape Town (UCT). Oxygen isotope ratios of whole rocks and quartz were determined using

conventional extraction methods after reaction with ClF_3. The O_2 was converted to CO_2 using a hot platinized carbon rod, and isotope ratios were measured using either a Finnigan MAT252 or a VG602E mass spectrometer and are reported in the familiar δ notation where $\delta=(R\text{sample}/R\text{standard}-1)\times 1{,}000$ and $R={}^{18}O/{}^{16}O$. The quartz standard NBS28 was run twice with each batch of eight samples, and the average difference between 18 pairs of NBS28 standards run during the course of this work was 0.13‰. This represents the typical precision of the analyses. Data were normalized to a value of NBS28 of 9.64‰, but the difference between normalized and unnormalized data is <0.5‰. Further details of the methods employed for extraction of oxygen from silicates at UCT are given by Vennemann and Smith (1990) and Harris et al. (2000). Wolframite, cassiterite, and hematite were analyzed using laser fluorination methods at UCT using the methods described by Harris et al. (2000). Replicate analyses of the Monastery garnet standard (Harris et al. 2000) suggest the precision is comparable to that of the conventional fluorination data. Unlike the conventional analyses, which comprise many individual grains, the laser data were obtained on individual mineral grains, and the yields were close to that expected for complete reaction.

Hydrogen isotopes were determined using the method of Vennemann and O'Neil (1993). Whole rock samples were degassed on the vacuum line at 200°C before pyrolysis. An internal water standard (CTMP, δD=−9‰) was used to calibrate the data to the standard mean ocean water (SMOW) scale and a second water standard DML (δD=−300‰) was used to correct for scale compression (e.g., Coplen 1993). Typical reproducibility of internal biotite standards during the period of analysis was ±2‰ (1 σ). Water contents were determined from the voltage measured on the mass 2 collector using identical inlet volume to standards of known number of micromoles. Repeated measurements of water standards of known mass suggest that the typical relative error for the water content is 3%.

Fluid inclusions in mineralized quartz vein samples from Brandberg West and Goantagab were analyzed for their H (and in the case of Brandberg West, C) isotope composition. Three grams of clean 5- to 9-mm chips of quartz vein were loaded into a 9-mm (inner diameter), oven-dried (800°C) quartz glass tube and attached to the vacuum line. The loaded sample was degassed at 50°C until no further rise in the pressure was noticed. The temperature was then increased gradually to 600°C causing the fluid inclusions to decrepitate, and the H_2O and CO_2 liberated from the sample were collected in a liquid nitrogen trap. The CO_2 was separated from the H_2O and CO_2 mix using an alcohol trap. The H-isotope composition of the H_2O was determined following procedures discussed above. The CO_2 was collected into an empty break-seal tube and analyzed using the same methods described below. In a detailed study of the isotope composition of fluids on a regional scale, Macey (2003) showed that neither the duration nor temperature (>300°C) of decrepitation had a significant effect on the δD values.

Carbon and oxygen isotope rations on carbonate host rock samples were determined after verifying the mineralogy by X-ray diffractometry. The limestones and marbles were found to consist almost entirely of calcite and quartz with little or no dolomite (<0.1%). Hence, CO_2 was extracted by reaction of 20 mg of powdered sample and 5 ml of 100% H_3PO_4 at 25°C. The CO_2 extracted from the calcite samples was analyzed for both carbon and oxygen and the data were corrected using the CO_2–calcite fractionation factor of 1.01025. An in-house carbonate standard, Namaqualand marble, was run with every five samples. The data obtained were used to convert the raw data to the PDB and SMOW scales.

Fluid inclusions

Nature of studied samples

Two greisen-type quartz–muscovite veins (Z94004Q and Z94006Q) from the Brandberg West Mine were selected for fluid inclusion analysis. Sample Z94004Q, (from a 50-cm wide vein) used for the microthermometric studies, consists dominantly of quartz with minor amounts of hematite (irregular anhedral habit), wolframite, and pyrite (cubic habit) and trace amounts of muscovite and epidote. The quartz is inequigranular (~0.5 to 5 mm) and shows only limited amounts of plastic strain in the form of weakly developed subgrain boundaries and sutured grain boundaries. Samples Z94004Q and Z94006Q gave indistinguishable microthermometric results; therefore, data from the two samples are presented together. Although only two samples were studied, the same fluid inclusion types were visible in other quartz veins related to the mineralization. The fact that essentially identical microthermometric data were obtained from the two different samples suggests that the fluid inclusion populations are representative of the quartz veins as a whole.

Fluid inclusions large enough for analysis are plentiful in the greisen-type quartz veins. Most often, the inclusions occur as subparallel sets of planar arrays, but isolated inclusions and clusters of inclusions are also fairly common. In general, each planar array or cluster of inclusions is relatively uniform with respect to inclusion characteristics (e.g., inclusion type, L/V, color). The majority of the fluid inclusions from the greisen-type veins are CO_2-rich, but aqueous inclusions were also observed. The two-phase undersaturated aqueous inclusions will be designated as type I inclusions and the three-phase CO_2-rich inclusions will be designated as type II. The relative chronology of the inclusion types is unclear, as the intersection relationships of fluid inclusion planes consisting of different types were equivocal. However, in some cases, type I and II inclusions were found together within the individual planar arrays. This suggests that they might represent immiscible fluid phases that were trapped at the same time, a possibility that will be evaluated below.

The type I aqueous inclusions contain a vapor bubble at room temperature occupying between 5 and 15 vol.% of the inclusion. The inclusions typically have anhedral, smoothly rounded ovoid, spherical, or tubular shapes, and most of the inclusions that were analyzed ranged in size from 4 to 17 μm with an average size of 8.5 μm. Several of the type I inclusions showed clathrate melting phenomena indicating the presence of a CO_2 component in the aqueous inclusions. The apparently pure aqueous inclusions are designated as type Ia, and those inclusions containing significant amounts of CO_2 are designated as type IIb. Except for showing clathrate melting, all type I inclusions have essentially identical microthermometric properties (Fig. 3; see below).

The type II carbonic inclusions are typically larger (<25 μm, mean=11.5 μm) than the aqueous inclusions; are either transparent or dark-colored; and have ovoid, spherical, rounded square, rounded rectangle, and negative crystal shapes. The type II inclusions can be divided into CO_2-rich (type IIb), which typically have volumetric CO_2/H_2O ratios between 0.8 and 0.95 at 20°C, and inclusions that contain approximately 30–40 vol.% CO_2 at 20°C (type IIa). These subtypes are present in roughly equal proportions. The proportion of liquid to vapor is variable and ranges from about 40% vapor to vapor-rich inclusions, where the proportion of liquid is impossible to estimate due to internal reflections.

Microthermometry

Microthermometry data are summarized in Table 1. The majority of the type I inclusions have eutectic melting temperatures (Te) between −46 and −22°C (mean −39, *n*=26). Although the accurate measurement of Te in such inclusions is not precise and some depression of melting could be due to hydrohalite melting, the uniformly low Te indicates the presence of significant divalent cationic species in the fluid inclusion solution. The divalent cation in the solution is most likely to be Ca^{2+} rather than Mg^{2+} or Fe^{2+} because of the availability of calcium in both plagioclase and the nearby marbles, which do not contain significant dolomite. Davis et al. (1990) suggested that inclusions with first melting temperatures<−37°C reflect the formation of metastable salt hydrates formed during freezing and do not necessarily indicate fluids that are rich in $CaCl_2$. The most likely model systems are, therefore, NaCl–$CaCl_2$–H_2O and NaCl–$CaCl_2$–H_2O–CO_2 and, even though significant R^{2+} cations are present, NaCl is most likely to be the dominant dissolved salt. The temperature of ice melting (Tm H_2O) for the type I aqueous inclusions ranges between −8.0 and −1.0°C, but most of the Tm H_2O values cluster around the mean of −5.5±1.1°C (Table 1). With the information available, it is not possible to estimate the $CaCl_2$/NaCl ratio of the inclusion fluids. If a $CaCl_2$–H_2O model system is assumed, the bulk salinity of the inclusions estimated from the Tm H_2O values and the phase diagram of Oakes et al. (1990) range from 2.0 to 11.9 wt%, with a mean of 8.7 wt% $CaCl_2$. If on the other hand, an NaCl–H_2O model system is assumed, the equation presented in Bodnar (1993) suggests a virtually identical range of salinity values from 1.8 to 11.7 wt% $NaCl_{equivalent}$, with a mean value of 8.6 wt% $NaCl_{equivalent}$. Roughly a third of the type I inclusions (type Ib) show clathrate melting (Table 1), which indicates the presence of dissolved CO_2. The Tm clathrate values are relatively tightly clustered around the mean of 6.7°C, which is equivalent to a salinity of 6.3 wt% equivalent NaCl, assuming the system is NaCl–H_2O–CO_2 using the equation of Diamond (1992a). These salinities are similar to the apparently CO_2-free type I inclusions. The type I inclusions have homogenization temperatures (Th) into the liquid phase of between 152 and 224°C, with a mean Th H_2O of 187±17°C (Fig. 3). The relatively narrow range in values shown in the bivariate plot of Th H_2O vs Tm H_2O (Fig. 3) suggests that the aqueous fluid phase represents a single fluid inclusion population. Th and Tm ice appear to show a vague negative correlation with r=−0.02, for the data set as a whole, and −0.57, for the type IIb inclusions. The latter correlation is only marginally significant at the 99% level; thus, it might indicate a mixing trend between two fluids having slightly different salinities.

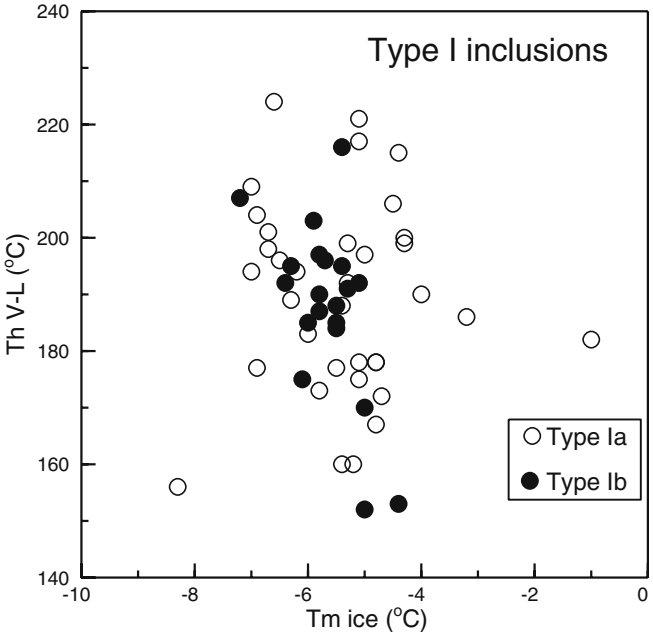

Fig. 3 Plot of homogenization temperature into the liquid (Th V–L) vs final melting temperature (°C) of ice for Type Ia and Ib inclusions. Ib inclusions show visible clathrate melting (see text)

The final melting of CO_2 (Tm CO_2) in the type II inclusions occurs between −61.0 and −56.6°C (Table 1; Fig. 4). No significant difference in Tm CO_2 was found between the CO_2-rich type IIb and CO_2-poor type IIa inclusions (Fig. 4). The depression of the triple point of pure CO_2 (−56.6°C) indicates the presence of other volatile species (e.g., CH_4, N_2, H_2S) in addition to the CO_2 (Roedder 1984; van den Kerkhof 1990). However, given that most of the inclusions have Tm CO_2 values between −56.6 and −59°C, only small amounts (<20 mol%) of additional components are likely (e.g., Parnell et al. 2000).

Table 1 Brandberg West mine: summary of microthermometric results for samples Z94004Q and Z94006Q

	N (quantity)	Range	Mean±SD		Range	Mean±SD
Type I aqueous inclusions						
Te H_2O (°C)	26	−46 to −23	Most −45 to −38	Model system	$NaCl–H_2O–CaCl_2–±CO_2$	
Tm H_2O (°C)	55	−8.0 to −1.0	−5.5±1.1	Salinity (wt% NaCl eq.)[a]	1.8 to 11.7	8.6±1.2
TmClath (°C)	20	5.6 to 8.0	6.7±0.7	Salinity (wt% NaCl eq.)[b]	3.9 to 8.0	6.2±1.2
Th H_2O (°C)	59	152 to 224	187.7±17.4	Density[c]	0.944	
Type II carbonic inclusions CO_2/H_2O=0.25 to 0.45						
Tm CO_2 (°C)	40	−61.0 to −56.7	−57.9±1.2	Model system	$NaCl–CaCl_2–H_2O–CO_2$	
TmClath (°C)	9	4.9 to 7.6	6.4±0.9	Salinity (wt% NaCl eq.)[b]	4.9 to 7.6	6.4±1.2
Th CO_2 (°C)	42	−2.0 to 26.3	15.7±7.2			
Type II carbonic inclusions: CO_2/H_2O=0.75 to 1.0						
Tm CO_2 (°C)	40	−60.3 to −56.6	−58.2±1.3	Model system	$NaCl–CaCl_2–CO_2±H_2O$	
TmClath (°C)	7	−2.0 to 4.6	2.1±2.7	Salinity (wt% NaCl eq.)[b]	9.6 to 17.5	13.1±3.8

[a]Salinity for a $CaCl_2–H_2O$ model solution determined using Tm H_2O and the equation of Oakes et al. (1990) are negligibly different from the values calculated assuming a NaCl–H_2O model system (i.e., $NaCl_{eq}$) using the equation of Bodnar (1993).
[b]Salinity was determined assuming a $NaCl–H_2O–CO_2$ model system using Tm Clath and the equation of Diamond (1992).
[c]Density was determined assuming mean salinity and mean Th H_2O.

The Th CO_2 values for the type II inclusions show a large range (−2.0 to 26.3°C). Tm clathrate values range from −2 to +7.6°C, with a mean value of 5.2°C, which is similar to the mean value obtained for the type Ib inclusions (6.7°C). Salinities of the type II inclusions estimated from the Tm Clath values must therefore be very similar to the type I, aqueous inclusions, assuming that they are approximated by the $NaCl–H_2O–CO_2$ system. This is consistent with the type I and II inclusions resulting from CO_2- and H_2O-rich immiscible, which developed from a single parent fluid. The type II inclusions decrepitate (at temperatures >350°C) before the total homogenization temperatures are reached. Here is a positive correlation (Fig. 4) between Th and Tm of the CO_2 component in type II inclusions, with r=0.69 for the whole population (n=84) and 0.79 and 0.57 for types IIa (n=41) and IIb (n=43), respectively. This suggests that the non-CO_2 volatile content is higher in those inclusions with highest density.

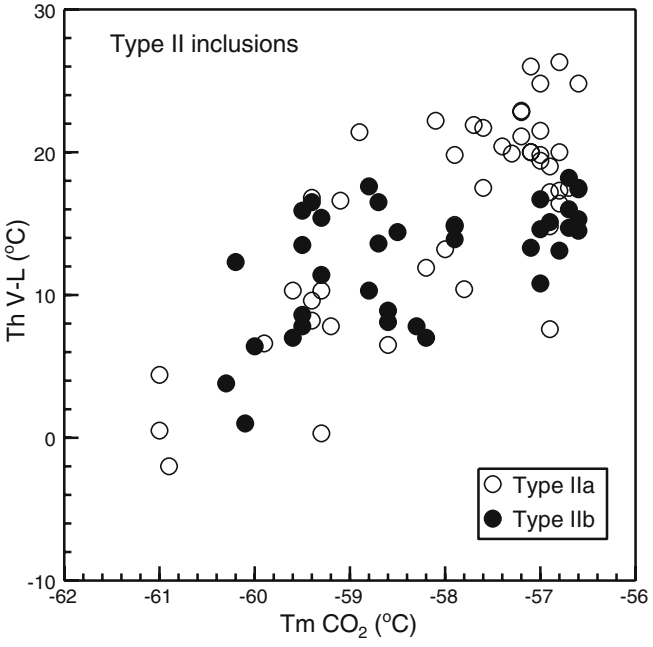

Fig. 4 Plot of homogenization temperature into the liquid (Th V–L) vs final melting temperature (°C) of CO_2 for Type IIa and IIb inclusions. IIb are CO_2-rich inclusions (CO_2/H_2O>0.5)

The presence of two different types of inclusion (types I and II), with similar salinities of the aqueous components, suggests that they might be related by immiscibility. Specifically, a homogeneous fluid in the system $H_2O–NaCl–CaCl_2–CO_2$ could have unmixed to form separate aqueous and carbonic fluids. The demonstration of such an unmixing process requires the coincidence of Th values for the two groups of inclusions (Ramboz et al. 1982), and unfortunately such data are lacking for the type II inclusions. Nevertheless, the presence of type I and II inclusions within the same inclusion trail is consistent with an origin via unmixing. Such a process could also explain the decrease in non-CO_2 component with decreasing density (Fig. 4) as CH_4 might be expected to be preferentially lost as the fluid "boiled" and vapor was lost from the system. The possible role of fluid immiscibility will be further discussed below.

Preliminary, unpublished microthermometric studies were carried out on the Frans, Goantagab, and Gamigab prospects by Petzel (1986) and Walraven (1988). These

studies suggest the Frans, Goantagab, and Gamigab prospects differ from the Brandberg West mine in having slightly higher salinities, lower Th H_2O values, and being dominated by NaCl and KCl rather than $CaCl_2$.

Stable isotopes

Regional patterns

The present research forms part of a larger study in which more than 400 O, H, and C isotope data have been obtained from the Zerrissene Group rocks, Pan African granitoids, and quartz veins with the principal aim of determining the nature and characteristics of fluid flow during the deformation, metamorphism, and plutonism in the Brandberg West area (Macey 2003). Several features of this data set are important in the context of the present paper and are summarized below and are presented in Figs. 5 and 6.

The slates, phyllites, and meta-graywackes of the Lower Ugab and Goantagab domains have $\delta^{18}O$ values ranging from 10.3 to 19.1‰ (n=66, mean=13.6±1.7‰, 1σ, n=62) and δD values that vary between −95 and −40‰ (n=66, mean=−68±12‰), with most values falling into a relatively narrow range of −82 to −47‰ (Macey 2003). These values are typical for low- to medium-grade metamorphosed sedimentary rocks (e.g., Sheppard 1986; Hoefs 1997). The carbonate rocks of the Lower Ugab domain have $\delta^{18}O$ values that range from 13.9 to 27.3‰ (n=47, mean=19.5±3.2‰, 1σ) and $\delta^{13}C$ values which range (Fig. 5) from −4.72 to + 6.72‰ (mean=1.2±3.0‰, 1σ). The calcite content of the marbles is high, with 75% of samples containing >80% calcite. There is no correlation between $\delta^{13}C$ value and weight percent of calcite, although those samples with <60% calcite tend to have $\delta^{13}C$<2‰ (Macey 2003). The range of $\delta^{13}C$ values is similar to that obtained for possible stratigraphic correlatives in the Otavi Group in central northern Namibia (e.g., Hoffman et al. 1998), which have been affected only by low-grade metamorphism. The $\delta^{18}O$ values of the marbles are generally lower than expected for marine carbonate rocks. The high calcite content and the lack of correlation between $\delta^{18}O$ and weight percent of calcite indicate that the low $\delta^{18}O$ values result from exchange with fluids rather than by decarbonation reactions during metamorphism.

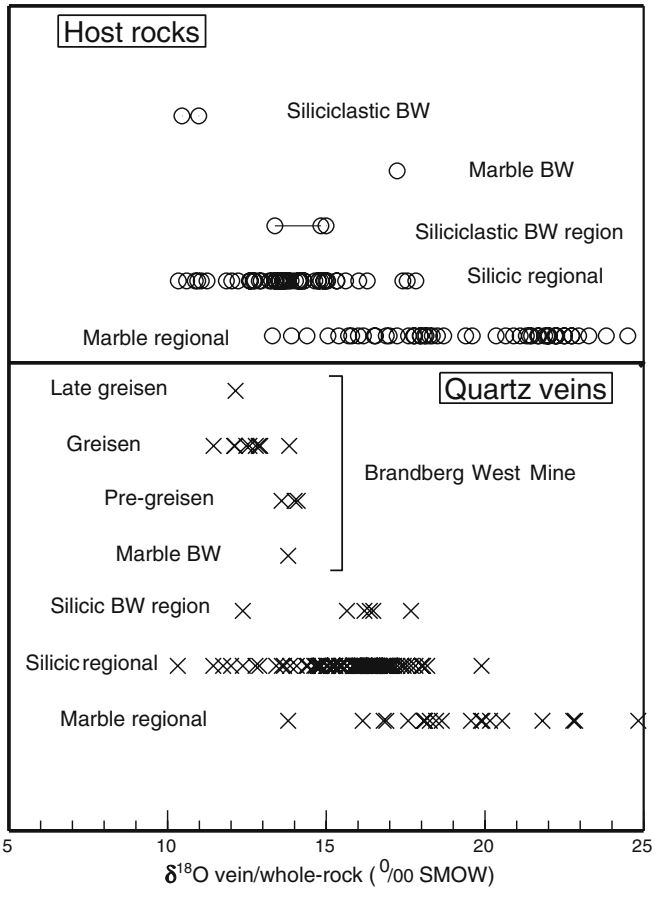

Fig. 5 Variation in $\delta^{18}O$ value of Brandberg West and regional host rocks and quartz veins. *BW* are samples from the mine, *BW region* are samples from the vicinity of the mine. Data from Table 1 and Macey (2003)

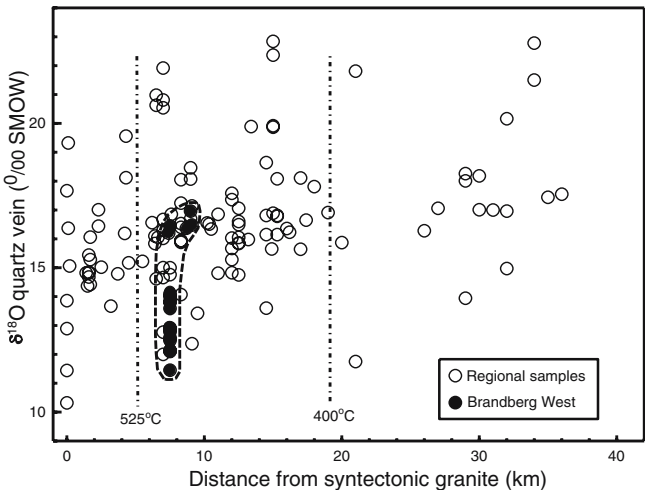

Fig. 6 Plot of quartz vein $\delta^{18}O$ value vs distance from the large mass of syn- and post-tectonic granites in the southern part of Fig. 1. As this is approximately perpendicular to the metamorphic isograds, the metamorphic grade decreases from *left* to *right* along the *x-axis*

The quartz veins hosted in the siliciclastic rocks have $\delta^{18}O$ values (Fig. 5) that vary regionally between 10.3 and 19.9‰ (n=115, mean=15.5±1.6‰), but most of the data have values between 14 and 18‰. The quartz veins hosted in carbonate rocks have $\delta^{18}O$ values ranging from 17.6 to 24.8‰ (n=24, mean=20.0±2.5‰). These values are significantly higher than the quartz veins hosted in the siliciclastic host rocks. The siliciclastic whole rock δD values vary between −95 and −40‰ (n=66, mean=−68±12‰), with most values falling into a relatively narrow range of −82 to −47‰ (Macey 2003). The variation of quartz vein $\delta^{18}O$ value across the Ugab Terrane is shown in Fig. 6. Quartz vein $\delta^{18}O$ shows a vague increase with increasing distance from the granites, with the lowest values in those veins in the immediate contact aureole of the granites. It is evident from Fig. 6 that the $\delta^{18}O$ values of quartz veins from the Brandberg West Mine area are lower

than is generally the case in the Ugab Terrane, and is comparable to quartz veins immediately adjacent to, and possibly genetically associated with, the granites.

The Pan-African Salem-type granites from around the Brandberg West area (Durissa, Mile 110, Voetspoor, Doros, and Central granites) have quartz $\delta^{18}O$ values between 10.8 and 14.8‰ (mean 12.4‰). Assuming a per mil difference between separated quartz and the original granite magma of 2‰ (e.g., Harris 1995), the average magma $\delta^{18}O$ value would have been 10.4‰, which is similar to the values (9.3 to 12.6‰) obtained for Salem granites from the northern central zone of the Damara Belt (Haack et al. 1982; Jung et al. 2000, 2003). These values are close to the boundary between I-type and S-type granites of 10‰ suggested by Harris et al. (1997). The δD values of biotite and hornblende in the Damaran granites range between −75 and −54‰, which are fairly typical for granitic rocks (e.g., Taylor and Sheppard 1986; Hoefs 1997).

Brandberg West and minor Sn–W deposits

The oxygen, carbon, and hydrogen isotope compositions of the veins and host rocks in and around the Brandberg West mine are given in Table 2. Figures 5 and 6 show that the oxygen isotope compositions of the hydrothermal quartz veins and wall rocks of the Brandberg West Sn–W deposit are distinct from the surrounding Zerrissene Group rocks and syn-tectonic veins. The two samples of siliciclastic host rock from within the pit have $\delta^{18}O$ values of 11.0 and 10.5‰, which are approximately 3–3.5‰ less than their counterparts from the surrounding unmineralized region. A quartz vein from outside the pit (Fig. 2), but within the main NE–SW trending band of quartz vein mineralization (Fig. 2), gave a $\delta^{18}O$ value of 12.4‰, which is similar to the greisen-type veins within the mine and significantly lower than the other analyzed veins (16.2 to 17.7‰) from the area surrounding the mine. The sample of Brandberg West Formation marble (Z94015HC) from within the mine has $\delta^{18}O$ and $\delta^{13}C$ values of 17.2 and 1.4‰, respectively (Table 2). These values are within the range obtained during the regional study (Fig. 5) and suggest that the carbonate rocks were not pervasively infiltrated by the ^{18}O-depleted hydrothermal fluids that altered the siliciclastic rocks. A quartz vein hosted in the Brandberg West Formation gave a $\delta^{18}O$ value of 13.8‰, which is significantly lower than the average for the regional carbonate-hosted quartz veins (20.2‰) and was most likely deposited from the mineralizing fluid.

Each of the phases of quartz vein formation identified in the Brandberg West mine have distinctive $\delta^{18}O$ values, which appear to become progressively ^{18}O-depleted as the veins become younger (Fig. 5). Although the early veins probably represent syn-orogenic veins, which predate the mineralizing fluids, they have quartz $\delta^{18}O$ compositions of between 13.6 and 14.1‰, which is approximately 2.5‰ less than the regionally occurring syn-orogenic veins (~16.5‰) sampled outside of the mineralized zone (Fig. 6). Most of the greisen veins have quartz $\delta^{18}O$ values of approximately 12.5‰ (range 11.5 to 12.8‰), suggesting that the $\delta^{18}O$ values of the early veins may have been partially reset by interaction with the main greisen mineralizing fluids. Analyses (Table 2) across a greisen-type vein (Z94012Q) reveal that the quartz at the edges of the vein, near the muscovite selvages, has higher $\delta^{18}O$-values (12.6‰) than at the core of the vein (11.5‰). The banded veins are morphologically and isotopically symmetrical (Table 2), suggesting that progressively younger quartz was deposited toward the center of the vein as the fracture widened during the multiple phases of fracturing followed by quartz deposition.

The $\delta^{18}O$ values of the wolframite, cassiterite, hematite, and muscovite from the greisen-type veins were determined for the purposes of isotope geothermometry, and the results are listed in Table 2. The oxide minerals gave very similar $\delta^{18}O$ values with wolframite (2.9 and 5.2‰), cassiterite (2.7 and 2.9‰), and hematite (1.8 and 2.0‰). Two muscovite samples both gave a $\delta^{18}O$ value of 9.9‰. These muscovite and oxide $\delta^{18}O$ values are similar to other hydrothermal vein-type deposits (e.g., Shieh and Zhang 1991). Carbon dioxide from the CO_2-bearing inclusions hosted in the cassiterite–wolframite-bearing quartz vein sample Z94004Q has a $\delta^{13}C$-value of 1.9‰. The isotope composition of the vein minerals and host rocks in and around the Frans and Goantagab deposits are listed in Table 3. The cassiterite-bearing quartz veins that occur at the Frans prospect have $\delta^{18}O$ values of 14.6 to 14.9‰. These values are about 2 to 2.5‰ higher than the Brandberg West mine quartz vein samples. The two hematite-rich quartz veins analyzed from the Goantagab mine have significantly different quartz $\delta^{18}O$ values of 18.1 and 14.1 (Table 3).

The siliciclastic rocks from within the Brandberg West, Frans, and Goantagab deposits have δD values of between −71 and −53‰, and the muscovite, which occurs as selvages along the margins of the greisen-type quartz veins, shows a relatively narrow range of δD values of −76 to −60‰ (Table 2). Unlike the oxygen isotopes at the Brandberg West deposit, the δD compositions of the siliciclastic rocks from the Sn–W deposits do not differ significantly from the regional δD patterns.

Discussion

Isotope geothermometry

At the Brandberg West Mine, the temperatures of greisen-vein formation were estimated from the oxygen isotope fractionation between the vein quartz and the muscovite selvages using the fractionation equation of Chacko et al. (1996). Quartz in contact with the muscovite selvages was used in preference to the quartz from the center of the veins to minimize the effects associated with the growth of multiple quartz generations, this being the pairing of minerals that most likely formed in equilibrium. The

Table 2 Isotopic composition of vein minerals and host rocks from the Brandberg West mine and surrounding area

Sample	Description	Mineral	$\delta^{18}O$	δD	$\delta^{13}C$	Vein classification
Quartz veins from mineralized zone						
Z94001Q	Qz–Cst–Hem–Cal	Cassiterite	2.9			Float sample
		Cassiterite	2.7			
Z94004Q	Qz–Wf–Py, Cu staining; mined	Quartz	12.5			Greisen-type vein
Z94005Q	Qz vein; not mined	Quartz	13.6			Early vein
Z94006Q	Qz–Ms–Hem–Wf–Ccp–Bn, Cu staining	Quartz	12.8			Greisen-type vein
		Wolframite	2.9			
		Wolframite	2.9			
		Hematite	2.0			
Z94008Q	Qz–Ms	Quartz	12.1			Greisen-type vein
Z94009Q	Qz–Ms–Hem	Quartz	12.9			Greisen-type vein
Z94011Q	Qz–Ms	Quartz	13.8			Greisen -type vein
		Muscovite		−66		
Z94012Qa	Qz–Ms–Hem + Cu staining	Quartz	12.6			Greisen -type vein
Z94012Qb	a and c = opposite edges	Quartz	11.5			
Z94012Qc	b = center, d = between edge and center	Quartz	12.9			
Z94012Qd		Quartz	12.3			
		Muscovite	9.9	−64		
		Muscovite	9.9	−61		
		Muscovite		−76		
		Hematite	1.8			
Z94013Q	S_1-parallel, hosted in carbonate rock	Quartz	13.8			Carbonate hosted
Z96215Q	Qz–Ms–Wf–Hem, Cu staining	Quartz	12.1			Greisen-type vein
		Muscovite	9.9	−60		
Z96217Q	S_1-parallel, Qz	Quartz	14.1			Early vein
Z96219Q	Qz–Hem	Quartz	14.0			Early vein
Z96222Q	Qz	Quartz	12.1			Late greisen vein
Z97003Q	Qz–Ms–Wf	Quartz	12.1			Greisen-type vein
		Wolframite	5.2			
Host rocks from the mineralized zone						
Z94003SH	Siliciclastic rock	Whole rock	11.0	−53		
Z94007SH	Siliciclastic rock	Whole rock	10.5	−71		
Z94015HC	Marble	Whole rock	17.2		1.41	
Quartz veins from the unmineralized surrounding area						
Z94183Q	Qz		16.2			Syn-orogenic
Z96210Q	Qz		16.4			Syn-orogenic
Z96213Q	Qz, Cu staining		12.4			Greisen vein
Z96214Q	Qz		16.5			Syn-orogenic
Z96223Q	Qz		17.7			Syn-orogenic
Host rocks from the unmineralized surrounding area						
Z96210SH	Siliciclastic rock		14.8	−72		
Z96214SH	Siliciclastic rock		15.0	−72		
Z97002(1)	Marble Brandberg W Fm.		19.4		−4.7	Contact Brak R Fm
Z97002(2)	Marble Brandberg W Fm.		20.4		0.5	
Z97002(5)	Marble Brandberg W Fm.		18.0		2.3	
Z97002(8)	Marble Brandberg W Fm.		16.0		0.2	
Z97002(9)	Marble Brandberg W Fm.		16.9		−1.2	
Z97002(11)	Marble Brandberg W Fm.		15.1		−2.7	
Z97002(11B)	Marble Brandberg W Fm.		18.0		−0.7	
Z97002(13)	Marble Brandberg W Fm.		18.1		−2.1	Contact Zebraputs
Fluid inclusions						
Z94004Q				−44	1.91	

Table 3 Isotopic composition of vein minerals and host rocks in and around the Frans prospect and the Goantagab mine

Sample number	Sample description	Mineral/rock	$\delta^{18}O$ (‰)	δD (‰)	$\delta^{13}C$ (‰)
Frans prospect: samples from the mineralized zone					
Z96163Q	Cassiterite-bearing Qz	Quartz	14.7		
	Ms greisen vein	Muscovite	12.8	−61	
Z96164Q	Cassiterite–quartz vein	Quartz	14.9		
Z96170Q	Qz–Ms greisen vein	Quartz	14.8		
Z96167HC	Calcitic marble	Whole rock	13.3		4.16
Unmineralized area surrounding Frans prospect					
Z96016Q	S_1-parallel quartz vein	Quartz	15.7		
Z96016SH	Siliciclastic rock	Whole rock	13.4	−63	
Z96038HC	Calcitic marble	Whole rock	21.9		5.96
Z96039HC	Calcitic marble	Whole rock	20.7		1.60
CHZ19	Calcitic marble	Whole rock	21.7		5.60
Z96169Q	S_1-parallel quartz vein	Quartz	15.4		
Z96162SH	Siliciclastic rock	Whole rock	13.4		
Z96166SH	Siliciclastic rock	Whole rock	13.7	−69	
Goantagab mining area: samples from the mineralized zone					
Z96187Qh	Hem-rich Qz vein float from mine workings	Quartz	18.1		
Z96187Qk	Hem-rich Qz vein float from mine workings	Quartz	14.1		
		Hematite	−0.7		
		Hematite	0.2		
Unmineralized area surrounding the Goantagab mining area					
Z96189Q	S_1-parallel syn-tectonic quartz vein	Quartz	13.6		
Z94195HC	Calcitic marble	Whole rock	25.4		3.98
Fluid inclusions Goantagab domain					
Z94218Q			15.8	−32	

Sample Z94218Q fluid inclusions analyzed by stepwise decrepitation for 10 min at 300, 400, 500, 600°C gave δD values of −34, −31, −32, and −30, respectively.

calculated temperatures range between 415 and 521°C with an average of 455±35°C (Table 4). The relatively large range in temperature estimates is to be expected given the small fractionation between muscovite and quartz at moderate to high temperatures. If an error of 0.1‰ is assumed for both mineral $\delta^{18}O$ values, the error for the temperature estimate is ±26°C. The temperatures determined using the quartz–muscovite isotope geothermometer are in relatively good agreement with the temperatures estimated from the thermal metamorphic mineral assemblages (Macey 2003; Goscombe et al. 2004).

Assuming isotope equilibrium, the coexisting quartz and hematite from within the greisen-type veins gave isotope equilibration temperatures of between 444 and 490°C (average 460°C), which are similar to the quartz–muscovite temperatures (Table 4). The only suitable cassiterite for analysis came from a single crystal found within the mine area, which had no adhering quartz. It was assumed that this mineral formed within a greisen vein and the maximum, minimum, and average $\delta^{18}O$ values of quartz from greisen veins has been used to calculate temperature in Table 4. The cassiterite–quartz isotope temperatures estimated in this manner, using the fractionation equation of Polyakov et al. (2005), range from 347 to 447°C (Table 4). The large oxygen isotope fractionation between both quartz and hematite, and quartz and cassiterite makes these mineral pairs effective isotope thermometers. For an error of 0.1‰ on both mineral $\delta^{18}O$ values, the error on the temperature estimate is ±9°C. Using the $\delta^{18}O$ value of quartz from the center of the greisen veins, which are lower, the temperatures estimated are very similar to the quartz–muscovite temperatures (Table 4).

If the quartz–cassiterite fractionation equation of Zheng (1991) is used, significantly lower temperatures are obtained (218–312°C). The isotope temperatures suggested by the quartz–wolframite pair for Z94006Q using the Zheng (1991) fractionation equations are 181 and 187°C (depending on which quartz $\delta^{18}O$ value is used) and 346°C for sample Z97003. The fact that relatively coherent temperatures are obtained for quartz–muscovite and quartz–cassiterite if the Polyakov et al. (2005) calibration is used for the latter pair, would seem to support their conclusions that the fractionation equations of Zheng (1991) give erroneously low temperatures. A similar

Table 4 Stable isotope geothermometry of the Sn–W deposits of the Brandberg West Area

Sample	Mineral pair	$\delta^{18}O_{Qz}$	$\delta^{18}O_{mineral}$	Temperature (°C, Eq. 1)	Temperature (°C, Eq. 2)
Brandberg West mine					
Z94001	Qz–Cst	11.5[a]	2.9	447 (Polyakov et al. 2005)	312 (Zheng 1991)
	Qz–Cst	(min)	2.7	438 (Polyakov et al. 2005)	302 (Zheng 1991)
	Qz–Cst	12.5[a]	2.9	400 (Polyakov et al. 2005)	269 (Zheng 1991)
	Qz–Cst	(ave.)	2.7	392 (Polyakov et al. 2005)	261 (Zheng 1991)
	Qz–Cst	13.8[a]	2.9	353 (Polyakov et al. 2005)	221 (Zheng 1991)
	Qz–Cst	(max)	2.7	347 (Polyakov et al. 2005)	218 (Zheng 1991)
Z94006	Qz–Wf	12.8	2.9	181 (Zheng 1992)	
	Qz–Wf	12.8	3.1	187 (Zheng 1992)	
	Qz–Hem	12.8	2	447 (Zheng 1991)	
Z94012	Qz–Hem	12.6	1.8	444 (Zheng 1991)	
	Qz–Hem	11.5	1.8	490 (Zheng 1991)	
	Qz–Ms	12.6	9.9	447 (Chacko et al. 1996)	
	Qz–Ms	12.6	9.9	451 (Chacko et al. 1996)	
	Qz–Ms	12.9	9.9	421 (Chacko et al. 1996)	
	Qz–Ms	12.9	9.9	415 (Chacko et al. 1996)	
Z96215	Qz–Ms	12.1	9.9	521 (Chacko et al. 1996)	
Z97003	Qz–Wf	12.1	5.9	346 (Zheng 1992)	
Goantagab mining area					
Z96187	Qz–Hem	14.1	0.2	347 (Zheng 1991)	
Z96187	Qz–Hem	14.1	−0.7	321 (Zheng 1991)	
Frans prospect					
Z96163	Qz–Ms	14.7	12.8	578 (Chacko et al. 1996)	

[a]Quartz values representing range found in greisen veins (maximum, minimum, and average quartz $\delta^{18}O$)

problem would, therefore, seem to be present in the Zheng (1992) equation for quartz–wolframite. Temperatures estimated for quartz–hematite pairs using the Zheng (1991) equation gives temperatures ranging from 444 to 490°C, which are consistent with the quartz–muscovite temperatures.

The quartz–muscovite isotope thermometry at the Frans prospect (578°C) revealed a temperature that is unrealistically high (Table 4) and might indicate a disequilibrium relationship between the quartz and muscovite. Coexisting quartz–hematite mineral pairs from the Goantagab deposit have an average oxygen isotope equilibration temperature of about 330°C, suggesting lower temperatures of vein formation than at Brandberg West.

Estimated pressure and temperature conditions of mineralization

Isochores for the type I aqueous inclusions were calculated assuming their composition is approximated by the NaCl–H_2O system using the Brown and Lamb (1989) equation of state, and a salinity of 8.6 wt% $NaCl_{equivalent}$ (Fig. 7). The isochores for the type II inclusions are more problematic to determine because of greater uncertainties of their densities and composition. In Fig. 7, they were calculated assuming a NaCl–H_2O–CO_2 system using the Bowers and Helgeson (1983) equation. The study of regional metamorphism by Goscombe et al. (2004) suggested that the maximum pressure experienced by the rocks in the Brandberg West area during the Damaran orogeny was in the vicinity of 2.5 to 3.2 kbar.

The quartz–muscovite isotope temperatures (415–451°C) are consistent with formation from the dense type IIb fluids (Th=15.7°C) at close to peak regional metamorphic pressures, but not compatible with the less dense type IIb fluids, whose isochores only reach a *P* of 2.5 kbar at temperaures >500°C. If the type I inclusion fluids and the low-density type II inclusions formed as a result of fluid unmixing, the intersection of the type I and II isochores suggests pressure–temperature conditions of about 1 kbar and 250°C. These temparature estimates are much more consistent with the quartz–cassiterite isotope temperatures (and to a lesser extent, the quartz–wolframite temperatures) determined using the Zheng (1991) equations, than the much higher temperatures obtained using the Polyakov et al. (2005) equation. However, this is not consistent with the quart–hematite isotope temperature obtained from the hematite-bearing veins, which represents the final stage of hydrothermal activity, and this gave isotope temperatures (447–490) that are much more consistent with the quartz–muscovite temperatures.

The concordant isotope temperatures obtained for quartz in equilibrium with muscovite, cassiterite, and hematite and the temperature suggested by the metamorphic mineral assemblage argue strongly that there was relatively little temperature decrease during the formation of the ore deposit. In any case, it is difficult to envisage how rapid

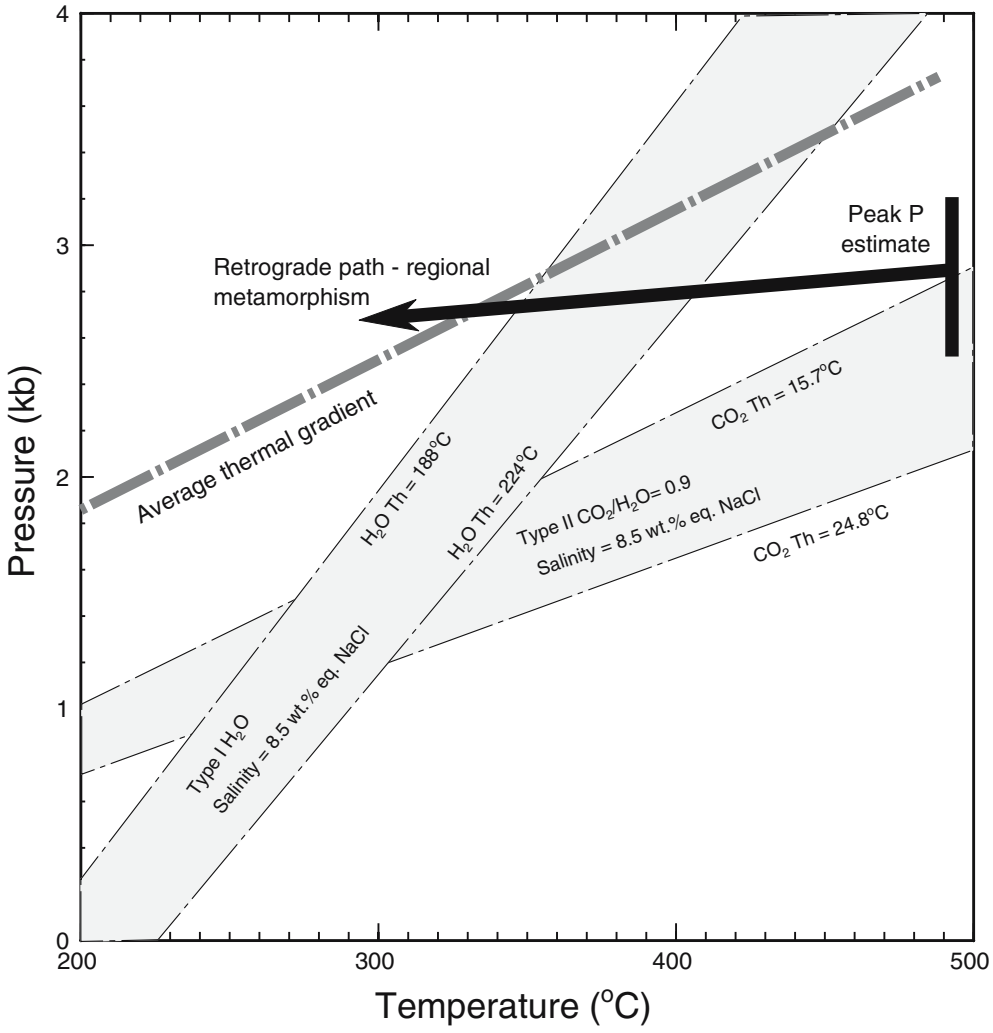

Fig. 7 P–T diagram showing isochores for type I and II inclusions encompassing the range of Th for each type. The pressure range for peak metamorphic conditions, the average thermal gradient at the time of metamorphism, and the cooling path post-regional metamorphism from Goscombe et al. (2004) are also shown

depressurization and cooling could have occurred in this situation where mineralization took place just after regional metamorphism at pressures of 2.5 to 3.2 kbar (~8–10 km depth). However, it is not obvious how this can be reconcliled with the lower temperatures obtained using the Zheng (1991, 1992) cassiterite and wolframite thermometers and the type II fluid inclusions. The pressure–temperature evolution of the ore forming fluids will be further discussed below.

Nature and origins of the mineralizing fluids

The fluids in equilibrium with the greisen muscovite from the Brandberg West mine have a range of δD compositions between −45 and −38‰ (Fig. 8), calculated using the muscovite–fluid fractionation equation of Suzuoki and Epstein (1976) and a temperature of 455°C. Analysis of the aqueous secondary fluid inclusions (extracted by decrepitometry) hosted in quartz vein sample Z94004Q from the Brandberg West mine yielded a δD value of −44‰, which is within the range of calculated fluid δD values for the greisen muscovite (Table 2). The $\delta^{18}O$ value of the Brandberg West mineralizing fluid was calculated using the quartz–water fractionation equation of Matsuhisa et al. (1979), assuming a temperature of 455°C, and yielded a range of values of 7.8 to 9.3‰ with a mean of 8.7±0.4‰ (n=11).

The $\delta^{18}O$ vs δD plot (Fig. 8) compares the composition of minerals from the Brandberg West deposits to those of granite, and the composition of the regionally metamorphosed siliciclastic country rocks are also shown. The Brandberg West deposit δD values are very similar to those of hydrous minerals from the granite. This is consistent with a magmatic origin for the fluids, but because the δD values of the siliciclastic rocks from within the Sn–W deposits do not differ from the regional δD values, it is not possible to exclude a model proposing a metamorphic fluid as the principal mineralizing fluid. However, lower $\delta^{18}O$ values of the mineralizing fluids would require that such a metamorphic fluid be derived from dehydration of rocks at the higher temperatures associated with thermal metamorphism as a result of nearby hidden granite.

It is also possible, at least on the basis of similarity of δD values, that the source of the fluids was meteoric. The O- and H-isotope composition of meteoric water at a

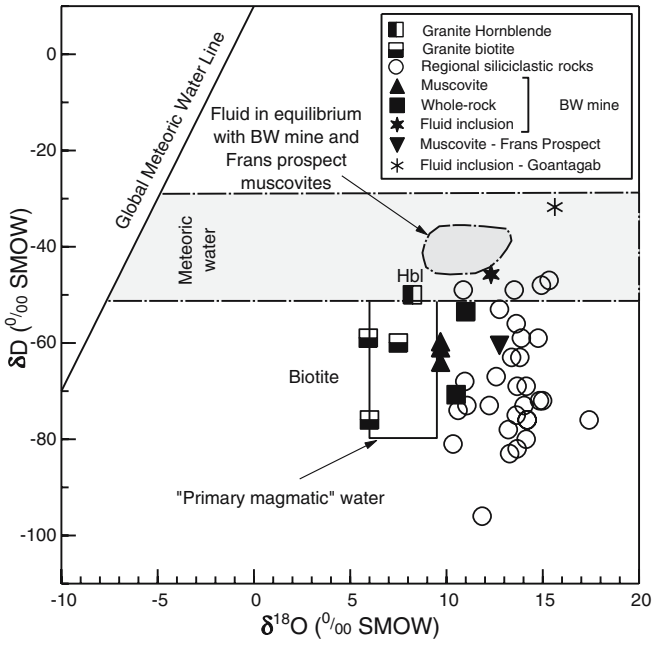

Fig. 8 Plot of δD vs δ^{18}O of Brandberg West Mine samples (muscovite), regional samples (whole rock), and Damara granites (biotite). Also shown is the field for "primary magmatic" water (Taylor 1977) and quartz vein fluid inclusion (δD by direct measurement, δ^{18}O estimated from quartz δ^{18}O value and quartz–water fractionation factor of Matsuhisa et al. 1979). The *shaded band* represents the range of values of meteoric water (−39±13 ‰, 1 SD) found at the present day at the equivalent latitude to Brandberg West at 530 Ma (see text). The *shaded field* indicates water in equilibrium with muscovite from BW and the Frans prospect, calculated assuming Δmusc–water (H)=−22.5 at 455°C (Suzuoki and Epstein 1976) and Δ musc–water (O)=0.5 (Chacko et al. 1996)

particular location depends on various physical parameters including latitude, altitude, and distance inland (Dansgaard 1964), of which only the first is known with any degree of certainty. The latitude of this region at the time of Damara granite intrusion (530–590 Ma) was about 39°S (Meert et al. 1995), and an estimate of the isotope composition of ambient meteoric water can be made by comparison with the data presented for modern rainfall by Rozanski et al. (1993). The average weighted mean δD value for rainfall of all the measuring stations between 34 and 44° N and S of the equator is −39‰ (±13, 1σ, n=29). This is the best estimate of the likely isotope composition of meteoric water and corresponds to a δ^{18}O value of −6.1‰ on the global meteoric water line (Fig. 8). The composition of the fluid in equilibrium with the Brandberg West deposit muscovites also has a δD value that matches the possible range of compositions of ambient meteoric water. However, at 455°C, quartz in equilibrium with meteoric water having a δ^{18}O value of −6.1‰ would have had a δ^{18}O value of −3.1‰, which is clearly much lower than the observed value. The lack of displacement of the Brandberg West deposit samples to low δ^{18}O values indicates that if any meteoric water is involved, it thoroughly equilibrated with the surrounding rocks along the flow path toward the zone of fluid–rock interaction.

Carbon dioxide from the CO_2-bearing inclusions hosted in the cassiterite–wolframite-bearing quartz vein sample Z94004Q has a δ^{13}C-value of 1.9‰. The CO_2 exsolved from mantle-derived magmas has δ^{13}C values of approximately −5 to −10‰, and sedimentary organic carbon typically has very negative δ^{13}C values of less than about −20‰ (Hoefs 1997). The fluid inclusion CO_2 does not contain a substantial component from either of these ^{13}C-depleted sources. If the temperature of vein formation were taken to be 455°C (from isotope geothermometry), the fluid inclusion CO_2 would have been in equilibrium with calcite having a δ^{13}C value of −1.9‰ (using the fractionation equation of Chacko et al. 1991). This value is lower than the mean (0.8‰), but within the range, of δ^{13}C value determined for the Brandberg West and Gemsbok River Formations (Macey 2003). These data indicate that the CO_2 was derived from the host carbonates. Batch thermal metamorphic decarbonation would produce CO_2 having a higher δ^{13}C than the whole rock carbonate, whereas acid dissolution ought to produce CO_2 with a similar δ^{13}C to the whole rock (assuming bulk dissolution, where the CO_2 liberated did not remain in equilibrium with the remaining host rock).

The apparent decrease in quartz δ^{18}O values from 12.9 to 11.5‰ toward the (younger) center of the Brandberg West mine greisen veins suggests that either the fluid δ^{18}O value or the temperature was changing during deposition of the vein material. Possible explanations for the decrease in δ^{18}O values of the quartz include:

1. The early greisen vein-forming fluids are likely to have interacted with the ^{18}O-enriched wall rocks, whereas later fluids would have passed through wall rocks that had at least partially equilibrated with the fluid.
2. The mineralizing fluid may have become progressively ^{18}O-depleted through an increase in the magmatic component in the fluid. This could have occurred as the magmatic fluid envelope displaced metamorphic fluids formed as a result of dehydration reactions during the early mineralization-related thermal metamorphism. Assuming a typical middle greenschist phyllitic rock assemblage that is 50% quartz and 50% biotite, the equations of Bottinga and Javoy (1973) for biotite–quartz and Matsuhisa et al. (1979) for quartz–water indicate that $\Delta_{\text{rock–water}}$ would have been about −0.2‰ at 455°C. Thus, fluid in equilibrium with the average siliciclastic rocks would have had a δ^{18}O value of 13.4‰. Any quartz vein forming from such a fluid should have a δ^{18}O value of 16.4‰ (assuming $\Delta_{\text{qz–water}}$=3.0, Matsuhisa et al. 1979), which is typical of the values observed in the regional veins.
3. Pirajno (1992) proposed that the hematization and carbonate alteration, which occurred during the final stages of mineralization, might have been associated with oxidizing meteoric fluids. This would have lowered the δ^{18}O value of the fluid and resulted in lower δ^{18}O values of precipitating quartz. However, the hydrogen isotope data do not support significant

involvement of meteoric water at Brandberg West (Fig. 8).

4. Unmixing of CO_2 from the fluid would lower the $\delta^{18}O$ value of the remaining aqueous component because of the large fractionation between CO_2 and water for oxygen. At 455°C, $\Delta_{CO2-water}$=6.2 (combining the calcite–water and CO_2–water fractionation factors of O'Neil et al. 1969 and O'Neil and Epstein 1966) and loss of 20% oxygen as CO_2 would lower the $\delta^{18}O$ value of the remaining fluid by 1.4‰, assuming a Rayleigh process.

The muscovite sample from the Frans prospect yielded a calculated fluid δD value of −27‰, and the quartz veins gave an estimated fluid $\delta^{18}O$ value at 375°C of 9.8±0.1‰ (n=3; using the equations of Suzouki and Epstein 1976 and Matsuhisa et al. 1979). An estimated $\delta^{18}O$ value of the Goantagab deposit mineralizing fluids of 7.9‰ was calculated using the quartz vein with a value of 14.1‰ and an equilibration temperature of 330°C.

If one assumes the quartz veins from the Frans prospect and Brandberg West mine were derived from a similar magmatic fluid source, the somewhat higher $\delta^{18}O$ values in the former could be due to lower temperatures of vein formation (as indicated by the absence of significant contact metamorphism) at the Frans prospect. Lower temperatures would mean larger quartz–water fractionation factors and would give higher quartz $\delta^{18}O$ values. The Gemsbok River Formation calcitic marble, which hosts part of the Frans deposit, has $\delta^{18}O$ and $\delta^{13}C$ values of 13.3 and 4.2‰, respectively. The $\delta^{18}O$ values are significantly lower (~8‰) than the average regional Gemsbok River Formation samples, which suggest interaction with comparatively ^{18}O-depleted mineralizing fluids. The higher quartz vein $\delta^{18}O$ values at the Frans prospect may therefore also be due to the fact that they may have developed from a fluid that (partially?) equilibrated with the ^{18}O-enriched carbonate rocks. The $\delta^{13}C$ value of the marble is typical for equivalent rocks in the Gemsbok River Formation away from the Sn deposit (Table 3) and would seem to indicate that there was little or no addition of magmatic CO_2.

At Goantagab, one quartz vein has a $\delta^{18}O$ value of 14.1‰, which like the Frans deposit, may indicate lower mineralization temperatures. The other analyzed quartz vein has a higher $\delta^{18}O$ value of 18.1‰, and this presumably reflects a strong rock buffering of the vein-forming fluid by the ^{18}O-enriched host carbonates (~25‰). In contrast to the Brandberg West mine and Frans prospect, the Goantagab quartz veins have higher $\delta^{18}O$ values than the unmineralized regional veins, which were sampled from the area surrounding the mine. However, this may just be due to the interaction of the mineralizing fluid with the carbonate rocks during the replacement-type mineralization.

Fluid–rock ratios

One of the principal applications of stable isotope geochemistry in ore deposit systems is to constrain the extent of fluid/rock interaction, and simple equations based on mass balance were defined by Taylor (1977). For the Brandberg West deposit, it can reasonably be assumed that the final $\delta^{18}O$ value of the altered host rock is 10.7‰ (the average of the two siliciclastic samples, Table 2), and that the initial $\delta^{18}O$ value of the host was 14.91‰ (the regional average). Assuming a typical middle greenschist phyllitic rock assemblage that is 50% quartz and 50% biotite, the equations of Bottinga and Javoy (1973) for biotite–quartz and Matsuhisa et al. (1979) for quartz–water indicates that $_{rock-water}$ would have been −0.2‰ at 455°C. If the average $\delta^{18}O$ value of the quartz veins in the mine is 12.3‰, then the $\delta^{18}O$ value of water in equilibrium with the veins at 455°C would have been 9.3‰ (using the fractionation equation of Matsuhisa et al. 1979). This suggests water/rock ratios of 1.88 (atomic units), assuming a closed system, and 1.06, assuming an open system. Although the models of Taylor (1977) have been superseded by more sophisticated models involving continuum mechanics (e.g., Baumgartner and Valley 2001), the mass balance approach still provides a semiquantitative estimate of how much isotope exchange has occurred. Therefore, the Brandberg West deposit appears to have experienced high, but plausible (when compared with other studies, e.g., Ren et al. 1992) fluid/rock ratios, which are consistent with its apparent proximal setting to the magmatic source body and the pervasive fluid infiltration of the host rocks.

Genesis of the Brandberg West area hydrothermal Sn–W deposits

The vast majority of greisen-type Sn–W deposits are spatially and genetically related to S-type granitic rocks (Pitcher 1979; Pirajno 1992; Burnham 1997). Evidence from several localities from around the world indicates that crystal/melt fractionation processes are not significant in enriching the tin concentrations in magmas, rather such enrichments would more likely result from the partial melting of a metal-enriched meta-sedimentary protolith (Burnham 1997). Geochemical analyses show that the Damaran meta-sedimentary rocks contain rare metals, especially tin, in concentrations at or greater than the crustal averages (Richards 1986). The Pan-African Salem-type and Ousis granites are considered to have become tin-rich during anatexis of these meta-sedimentary rocks (de Waal 1986; Walraven 1989). Recent work by Jung et al. (2000, 2003) has confirmed a crustal origin for these granites. The Brandberg West area Sn–W deposits may therefore have developed from strongly differentiated, tin-rich residual magmatic fluid derived from the tin-enriched S-type Damara granites. Alternatively, the magmas provided only the heat, and the tin deposits developed by the formation of hydrothermal convection cells surrounding the plutons and would have used the orogenic/metamorphic fluids to scavenge and transport the tin. As discussed above, the O and H isotopes suggest that the Sn–W deposits were derived from mineralizing fluids, which contained a strong igneous component, and the magmatic model appears to be

the more likely. Other possible models include mixing of meteoric water with fluids of metamorphic origin and imperfect isotopic buffering of meteoric water by country rocks in a transient convective system related to a granite intrusion. However, as discussed above and illustrated in Fig. 8, significant quantities of unmodified meteoric water were not involved in the genesis of the Brandberg West ore deposit.

Pirajno et al. (1992/93) reported that the sulfides at the Brandberg West mine (pyrite and chalcopyrite) and the Goantagab prospect (pyrite, sphalerite, pyrrhotite) have $\delta^{34}S$ values between 0.9 and 1.3‰ and 4.8 and 6.3‰, respectively (relative to Canyon Diablo troilite). These values are very similar to the $\delta^{34}S$ values (−1.2 to 3.8‰) obtained for the granite-related mineralization of the central zone of the Damara Belt (Pirajno et al. 1992/93). The sulfide samples from the Brandberg West mine have $\delta^{34}S$ values close to primitive mantle composition (0‰), suggesting a magmatic, igneous source for the sulfur. The higher $\delta^{34}S$ values obtained at the Goantagab deposit most likely indicate a mixing of magmatic fluids and crustal material, probably during the hydrothermal replacement (Pirajno et al. 1992/93).

Based on the geological and geochemical characteristics of the mineralization, Pirajno and Jacob (1987b) and Walraven (1989) propose that the four main deposits in the Brandberg West area, the Brandberg West, Frans, Goantagab and Gamigab deposits were emplaced at progressively higher levels above their source granite cupolas (Fig. 9). The well-developed greisenization, the association of W and Sn, and the paucity of sulfide minerals led Pirajno and Jacob (1987b) to interpret the Brandberg West deposit to be the most proximal of the deposits. In contrast, the relatively minor quantities of W, the abundance of sulfides, and its replacement-type character led Pirajno and Jacob (1987b) to suggest the Goantagab prospect is the most distal of the deposits. Assuming they were derived from the same mineralizing fluid, the progressively higher oxygen isotope values obtained for quartz veins at the Brandberg West, Frans, and Goantagab deposits suggest that they were deposited at progressively lower temperatures, which is consistent with them being more distal to their magmatic source than the Brandberg West deposit and supports the Pirajno and Jacob (1987b) model.

The deposition of metals from ore solutions occurs due to the reduction in the stability of metal-transporting chloride complexes, which usually result from one or more factors including changes in the temperature, pressure, fluid immiscibility and boiling, mixing with other fluids, physical barriers, chemical reactions with country rocks (Guilbert and Park 1986; Pirajno 1992; Barnes 1997). Changes in temperature may occur as the

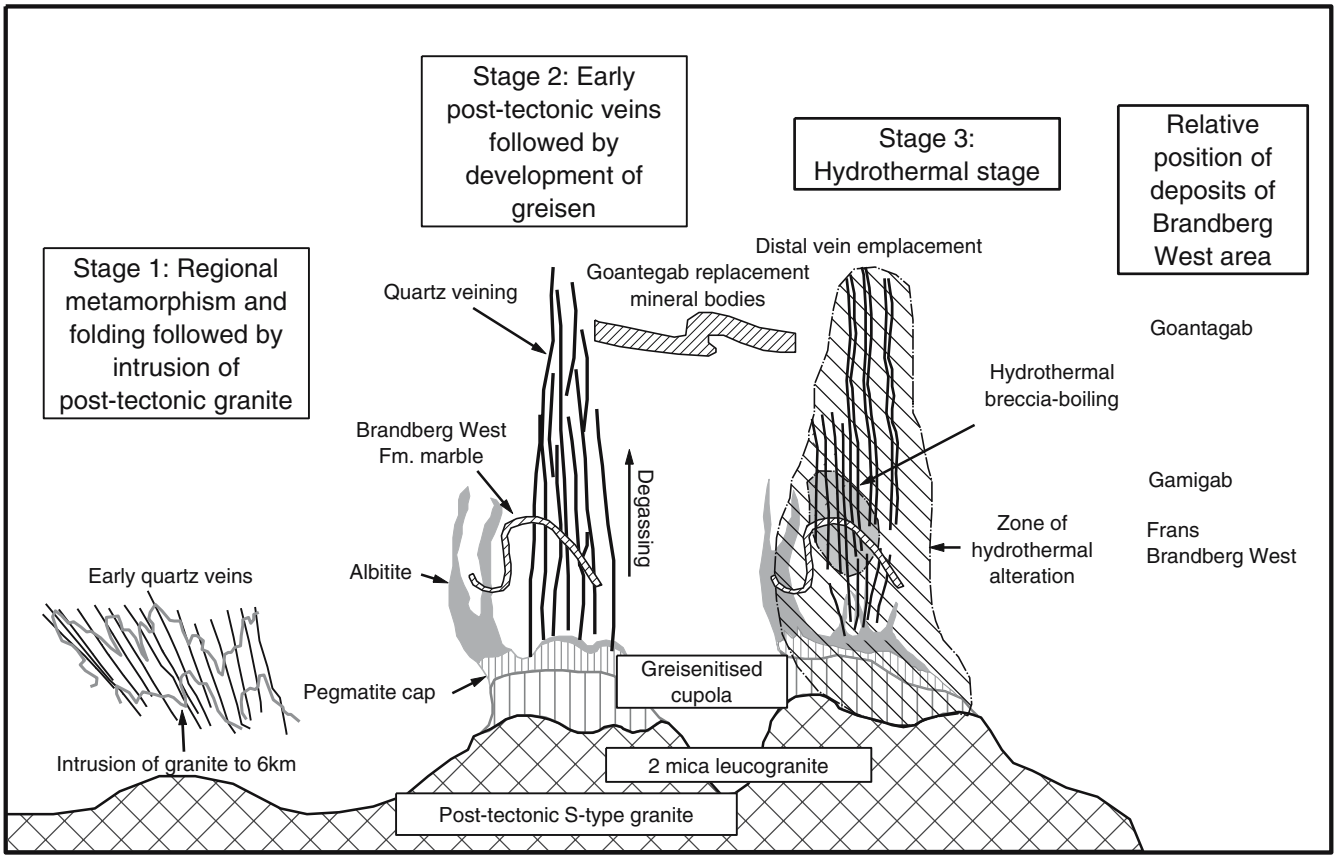

Fig. 9 Schematic diagram showing the evolution of the Brandberg West deposits modified after Pirajno (1992). The relative positions of the Brandberg west deposit and other deposits in the area are indicated

fluid moves through cooler host rock and mixes with cooler groundwaters and/or thermal expansion but are rarely considered to be the direct cause of metal deposition in hydrothermal deposits since a fairly rapid decrease of at least 20°C is needed to produce a spatially restricted deposit. The fluid inclusion study of the Brandberg West deposit indicates that the deposition of the Sn and W oxides may have been associated with phase separation (type I and II inclusions). According to Roedder (1984), such effervescence is a particularly effective mechanism for ore deposition. However, no unambiguous evidence for boiling (Roedder 1984, p 256) was observed during the fluid inclusion study. In an isotope study of a greisen-type tin deposit in Russia, Sushchevskaya and Borisov (1992) concluded that the cassiterite mineralization can occur at the mixing interface of alkaline meteoric waters and Sn-bearing acidic chloride solutions. The δD values of the Sn–W deposit fluids suggest meteoric water was not a dominant fluid during the formation of the Brandberg West deposit.

Most of the main Sn–W deposits of the Brandberg West area are located at the interface of siliciclastic and carbonate units. As already discussed, the siliciclastic host rocks at Brandberg West have lower δ^{18}O values than normally found in the Lower Ugab Domain due to pervasive interation with the ^{18}O-depleted mineralizing fluid. In contrast, the oxygen isotope compositions of the carbonate host rocks have not been lowered by the mineralizing fluid, suggesting that the marbles have not undergone significant pervasive fluid–rock interaction. Furthermore, there is no C-isotope evidence for extensive exchange with magmatic CO_2, which typically has δ^{13}C values of between −5 and −10‰ (e.g., Hoefs 1997). A quartz vein hosted in the carbonate horizon capping the Brandberg West deposit yielded a δ^{18}O value significantly lower than the average for the regional carbonate-hosted quartz veins and was clearly derived from the mineralizing fluid. The stable isotope composition of the carbonates and their quartz veins, therefore, indicates that unlike the siliciclastic host rocks, the mineralizing fluid flow was channeled along fractures in the carbonates. The lack of pervasive flow through the carbonates and the general paucity of quartz veins crosscutting the carbonate rocks argue strongly that the Brandberg West Formation rocks acted as barriers to fluid migration during the formation of the deposit. This may be expected since the marbles are ductile, contain few joints and fractures, and have been completely recrystallized, rendering them largely impermeable.

As already shown, the δ^{13}C of fluid inclusions indicate that the greisen-type mineralized veins in the Brandberg West mine contain CO_2, which was derived from host rock carbonates, indicating some interaction between the marbles and the mineralizing fluids. This suggests that the carbonate rocks may have not only provided a physical barrier, but may have caused ore deposition through chemical reactions. One such reaction, which could have produced CO_2, is the acid dissolution reaction that could be associated with a change in the pH of the mineralizing fluid, causing the destabilization of the Sn- and W-chloride complexes and the precipitation of cassiterite and wolframite (Pirajno 1992).

Conclusions

1. Sn–W mineralization at Brandberg West occurred via CO_2 bearing moderately saline aqueous fluids belonging to the system NaCl–$CaCl_2$–H_2O–CO_2.
2. The temperature of mineralization based on quartz–mineral oxygen isotope fractionations was between about 390 and 520°C, whereas fluid inclusions suggest somewhat lower temperatures. The Polyakov et al. (2005) fractionation equations for cassiterite give temperatures that are consistent with quartz–muscovite and quartz–hematite temperatures.
3. Stable isotope data for quartz veins and host rocks in the area of the mine suggest that the host rock δ^{18}O values have been lowered by interaction with fluids. The quartz veins have δ^{18}O values that are similar to quartz veins at the contact of syntectonic Damara-age granites to the south.
4. The similarity of oxygen- and hydrogen-isotope data for the quartz–muscovite veins and the nearby granites indicates that the fluids are magmatic in origin and that the mineralization is probably in the cupola of a hidden granite intrusion, as suggested by previous authors (Pirajno et al. 1987, 1992/93).
5. The CO_2 component of the mineralizing fluid has δ^{13}C values that are consistent with its derivation by dissolution of marble.
6. It is most likely that the Brandberg West Sn–W deposit was formed where relatively impermeable marbles formed a barrier to the passage of magmatic fluids and reacted with the fluid. The Ca^{2+} and CO_2 seen in the fluid inclusions were derived from the marble. The water to rock ratios calculated by simple mass balance methods were between 1 and 1.9 (atomic units) for an open and closed system, respectively.
7. Minor uneconomic deposits in the region show similar features but with lower quartz vein δ^{18}O values. These data are consistent with the suggestion of Pirajno et al. (1987,1992/93) that they represent mineralization at greater heights above hidden granite plutons.

Acknowledgements We are grateful to the National Research Foundation for financial support via a grant to CH and a post-graduate bursary to PM. Andrew Menzies is thanked for assistance in the field. Help with the analytical work was provided by Fayrooza Rawoot and John Lanham. Eric Bryce, Bruce Cairns, and Charlie Ledger provided invaluable assistance in setting up the laser fluorination system. We also thank Franco Pirajno, an anonymous reviewer, and associate editor Christian Marignac for providing detailed and helpful reviews.

References

Barnes HL (1997) Geochemistry of hydrothermal deposits, 3rd edn. Wiley, New York, p 795

Baumgartner LP, Valley JW (2001) Stable isotope transport and contact metamorphic flow. In: Valley JW, Cole DR (eds) Stable isotope geochemistry. Rev Mineral Geochem 43:415–467

Bentley PN (1985) Granitoid related Sn–W mineralization, with special reference to Southern Africa, the Variscan Belt in Europe and the Malay Peninsula. Dissertation, Rhodes University, Grahamstown

Bodnar RJ (1993) Revised equation and table for determining the freezing point depression of H_2O–NaCl solutions. Geochim Cosmochim Acta 57:683–684

Bottinga Y, Javoy M (1973) Comments on oxygen isotope geothermometry. Earth Planet Sci Lett 20:250–265

Bowen MP (1984) Short report—review of the potential for economic tin discoveries in the Brandberg West area, with reference to stream sediment and lithosampling results. Gold Fields Namibia internal report, p 12

Bowen MP, Evers T (1989) Lithogeochemistry as a tool for extending mineral resources; the Brandberg West Sn–W deposit, Damaraland, South West Africa/Namibia. J Geochem Exploration 34:47–62

Bowers TS, Helgeson HC (1983) Calculation of the thermodynamic and geochemical consequences of non-ideal mixing in the system H_2O–CO_2–NaCl on phase relations in geologic systems: equations of state for H_2O–CO_2–NaCl fluids at high pressures and temperatures. Geochim Cosmochim Acta 47:1247–1275

Brown PE, Lamb WM (1989) P–V–T properties of fluids in the system H_2O–CO_2–NaCl: new graphical presentations and implications for fluid inclusion studies. Geochim Cosmochim Acta 53:1209–1221

Burnham CW (1997) Magmas and hydrothermal fluids. In: Barnes HL (ed) Geochemistry of hydrothermal deposits, 3rd edn. Wiley, New York, pp 63–123

Chacko T, Mayeda TK, Clayton RN, Goldsmith JR (1991) Oxygen and carbon isotope fractionation between CO_2 and calcite. Geochim Cosmochim Acta 55:2867–2882

Chacko T, Hu X, Mayeda TK, Clayton RN, Goldsmith JR (1996) Oxygen isotope fractionations in muscovite, phlogopite and rutile. Geochim Cosmochim Acta 60:2595–2608

Coplen TB (1993) Normalisation of oxygen and hydrogen isotope data. Chem Geol 72:293–297

Dansgaard W (1964) Stable isotopes in precipitation. Tellus 16:436–468

Davis DW, Lowenstein TK, Spencer RJ (1990) Melting behaviour of fluid inclusions in laboratory-grown halite crystals in the system NaCl–H_2O, NaCl–KCl–H_2O, NaCl–$MgCl_2$–H_2O and NaCl–$CaCl_2$–H_2O. Geochim Cosmochim Acta 54:591–601

de Waal SA (1986) The stanniferous Ousis granite, precursor magma of the Uis pegmatites, Uis, South West Africa. Fortschr Mineral 64:135–149

Diamond LW (1992) Stability of CO2 clathrate hydrate + CO_2 liquid + CO_2 vapour + aqueous KCl–NaCl solutions: experimental determination and application to salinity estimates of fluid inclusions. Geochim Cosmochim Acta 56:273–280

Diehl M (1990) Geology, mineralogy, geochemistry and hydrothermal alteration of the Brandberg Alkaline Complex, Namibia. Geological Survey Namibia Memoir 10:1–11

Diehl BJM (1992a) Tin. In: The mineral resources of Namibia. Geological Survey of Namibia, Windhoek, pp 2.8–1 to 2.8–24

Diehl BJM (1992b) Tungsten. In: The mineral resources of Namibia. Geological Survey of Namibia, Windhoek, p 2.9–2

Elliot L (1985) The wall rocks of the Brandberg west Open pit, Namibia. Thesis, Rhodes University, Grahamstown

Evers T, Bowen MP (1989) Lithogeochemistry as a tool for extending mineral resources; the Brandberg West Sn–W deposit, Damaraland, South West Africa/Namibia. J Geochem Explor 34:47–62

Frimmel HE, Hallbauer DK, Gartz VH (1999) Gold mobilizing fluids in the Witwatersrand basin: composition and possible sources. Mineral Petrol 66:55–81

Goscombe B, Gray D, Hand M (2004) Variation in metamorphic style along the Northern Margin of the Damara Orogen, Namibia. J Petrol 45:1261–1295

Guilbert JM, Park CF (1986) The geology of ore deposits. Freeman, San Francisco, CA, p 985

Haack U, Hoefs J, Gohn E (1982) Constraints on the origin of Damaran granites by Rb/Sr and $\delta^{18}O$ Data. Contrib Mineral Petrol 79:279–289

Hälbich IW, Freyer EE (1985) Structure and metamorphism of Damaran rocks in the Ugab profile, Progress Report for 1982/83. Commun Geol Surv Namib 1:97–99

Harris C (1995) Oxygen isotope geochemistry of the Mesozoic anorogenic complexes of Damaraland, northwest Namibia: evidence for crustal contamination and its effect on silica saturation. Contrib Mineral Petrol 122:308–321

Harris C, Faure K, Diamond, RE Scheepers R (1997) Oxygen and hydrogen isotope geochemistry of S- and I-type granitoids: the cape granite suite, South Africa. Chem Geol 143:95–114

Harris C, Smith S, le Roex AP (2000) Oxygen isotope composition of phenocrysts from Tristan da Cunha and Gough Island lavas: variation with fractional crystallization and evidence for assimilation. Contrib Mineral Petrol 138:164–175

Hoefs J (1997) Stable isotope geochemistry. Springer, Berlin Heidelberg New York, p 201

Hoffmann KH (1987) Application of tectonostratigraphic terrane analysis in the Damara Province of central and northern Namibia. In: Abstract Volume, AL du Toit golden jubilee conference on tectonostratigraphic terrane analysis, Royal Society and Geological Society of South Africa, Cape Town, pp 25–27

Hoffman PF, Hawkins DP, Isachsen CE, Bowring SA (1996) Precise U–Pb zircon ages for early Damaran magmatism in the Summas Mountains and Welwitschia inlier, northern Damara belt, Namibia. Commun Geol Surv Namib 11:47–52

Hoffman PF, Kaufman AJ, Halverson GP, Schrag DP (1998) A Neoproterozoic snowball earth. Science 281:1342–1346

Hu G, Clayton RN, Polyakov VB, Mineev SD (2005) Oxygen isotope fractionation involving cassiterite (SnO_2) II: determination by direct exchange between cassiterite and calcite. Geochim Cosmochim Acta 69:1301–1305

Jacob RE, Kruger FJ (1994) Age of hydrothermal tin mineralization in the region northwest of the Brandberg, Namibia. In: Abstract Volume, Proterozoic crustal and metallogenic evolution, Geological Society and Geological Survey of Namibia, p 34

Jeppe JFB (1952) The geology of the area along the Ugab River, west of the Brandberg. Thesis, University of Witwatersrand, Johannesburg, pp 224

Jung S, Hoernes S, Mezger K (2000) Geochronology and petrogenesis of Pan-African, syn-tectonic, S-type and post-tectonic A-type granite (Namibia): products of melting of crustal sources, fractional crystallization and wallrock entrainment. Lithos 50:259–287

Jung S, Mezger K, Hoernes S (2003) Petrology of basement-dominated terranes: II. Contrasting isotopic (Sr, Nd, Pb and O) signatures of basement-derived granites and constraints on the source region of granite (Damara orogen, Namibia). Chem Geol 99:1–28

Macey PH (2003) The characteristics of regional-scale fluids, fluid-flow and hydrothermal mineralization in meta-sedimentary terranes: a stable isotope and fluid inclusion study of the Zerrissene Group meta turbidites and Sn–W deposits, Brandberg West area, Neoproterozoic Damara Orogen, central western Namibia. PhD Thesis, University of Cape Town, p 332

Maclaren AH (1993) The structural control of tin mineralization in the Goantagab mining area and surrounding grant, Damaraland, Namibia. Abstract, Mineral Exploration '93, Cape Town

Matsuhisa Y, Goldsmith JR, Clayton RN (1979) Oxygen isotope fractionation in the system quartz–albite–anorthite–water. Geochim Cosmochim Acta 43:1131–1140

Meert JG, Van der Voo R, Ayub S (1995) Paleomagnetic investigation of the Neoproterozoic Gagwe lavas and Mbozi complex, Tanzania and the assembly of Gondwana. Precambrian Res 74:225–244

Miller RMcG (1983) The Pan-African Damara orogen of South West Africa/Namibia. In: Miller RMcG (ed) Evolution of the Damara orogen of South West Africa/Namibia. Spec Publ Geol Soc S Afr 11:431–515

Miller R McG (1992) Mineral exploration targets in Namibia. In: The mineral resources of Namibia. Geological Survey of Namibia, Windhoek, pp 1.1–1 to 1.1–5

Milner SC (1997) Geological map of Omaruru. Sheet 2114. 1:250000. Geological Survey of Namibia, Windhoek

Oakes CS, Bodnar RJ, Simonson JM (1990) The system NaCl–$CaCl_2$–H_2O: I. The ice liquidus at 1atm total pressure. Geochim Cosmochim Acta 54:603–610

O'Neil JR, Epstein S (1966) A method for the oxygen isotope analysis of milligram quantities of water and some of its applications. J Geophys Res 71:4955–4961

O'Neil JR, Clayton RN, Mayeda TK (1969) Oxygen isotope fractionation in divalent metal cations. J Chem Phys 51:5547–5558

Osborn RI (1985) Regional mapping of Brandberg North (portions of grants 1068, 1299 and 1300). Gold Fields Namibia internal report, p 16

Parnell J, Earls G, Wilkinson JJ, Hutton DHW, Boyce AJ, Fallick AE, Ellam RM, Gleeson SA, Moles NR, Carey PF, Legg I (2000) Regional fluid flow and gold mineralization in the Dalradian of the Sperrin Mountains, Northern Ireland. Econ Geol 95:1389–1416

Petzel VFW (1986) Vein and Replacement type Sn and Sn–W Mineralization in the Southern Kaoko Zone, Damara Province, South West Africa/Namibia. Thesis, Rhodes University, p 141

Pirajno FMC (1992) Hydrothermal mineral deposits. Springer, Berlin Heidelberg New York, p 311

Pirajno FMC, Jacob RE (1987a) Hydrothermal tin–tungsten mineralization in the Brandberg West–Goantagab area of the Damara Orogen, South West Africa/Namibia. Commun Geol Surv Namib 3:99–103

Pirajno FMC, Jacob RE (1987b) Sn–W metallogeny in the Damara Orogen, South West Africa/Namibia. S Afr J Geol 90:239–255

Pirajno FMC, Petzel VFW, Jacob RE (1987) Geology and alteration-mineralization of the Brandberg West Sn–W deposit, Damara Orogen, South West Africa/Namibia. S Afr J Geol 90:256–269

Pirajno FMC, Kinnaird JA, Fallick AE, Boyce AJ, Petzel VWF (1992/93) A preliminary regional sulphur isotope study of selected samples from mineralised deposits of the Damara Orogen, Namibia. Commun Geol Surv Namib 8:81–97

Pitcher WS (1979) Comments on the Geological environments of granites. In: Atherton MP, Tarney J (eds) The origin of granite batholiths: geochemical evidence, Shiva, Cheshire, UK, pp 1–44

Polyakov VB, Mineev SD, Clayton RN, Hu G, Gurevich DA, Khramov KS, Gavrichev VE, Gorbunov VE, Golushina LN (2005) Oxygen isotope fractionation involving cassiterite (SnO_2) I: calculation of reduced partition function ratios from heat capacity and X-ray resonant studies. Geochim Cosmochim Acta 69:1287–1300

Potgieter JE (1984) Progress report on exploration conducted on the Frans Prospect during the period October 1982 to May 1983. Grant M46/3/1380 (Brandberg North Project). Gold Fields Namibia internal report, p 8

Ramboz C, Pichavant M, Weisbrod A (1982) Fluid immiscibility in natural processes: use and misuse of fluid inclusion data. Chem Geol 37:29–48

Ren Q, Zhang C, Yang R, Xie X, Xu Z (1992) Hydrothermal systems related to epithermal gold deposits in Mesozoic volcanic areas in eastern China. In: Kharaka and Maest (eds) Water–rock interaction. Balkema, Rotterdam, pp 1609–1612

Richards TE (1986) Geological characteristics of rare-metal pegmatites of the Uis type in the Damara Orogen, SWA/Namibia, 1845–1862. In: Anhausser CR, Maske S (eds) Mineral deposit of Southern Africa, vols. 1 and 2. Geological Society of South Africa, Johannesburg

Roedder E (1984) Fluid inclusions. Reviews in mineralogy, vol. 12. Mineralogical Society of America, Washington, DC, p 644

Rozanski K, Araguas-Araguas L, Gonfiantini R (1993) Isotopic patterns in Global Precipitation. Geophysical monograph 78, American Geophysical Union, pp 1–35

Seth B, Kröner A, Mezger K, Nemchin AA, Pidgeon RT, Okrusch M (1998) Archaean to Neoproterozoic magmatic events in the Kaoko belt of NW Namibia and their geodynamic significance. Precamb Res 92:341–363

Sheppard SMF (1986) Characterisation and isotopic variations in natural waters. In: Valley JW, Taylor HP, O'Neil JR (eds) Stable isotopes in high temperature geological processes. Reviews in Mineralogy, vol. 16. Mineralogical Society of America, pp 1–12

Shieh Y-N, Zhang G-X (1991) Stable isotope studies of quartz-vein type tungsten deposits in Dajistan mine, Jiangxi Province, southeast China. In: Taylor HP, O'Neil JR, Kaplan JR (eds) Stable isotope geochemistry: a tribute to Samuel Epstein. The Geochemical Society Special Publication 3, pp 425–435

Sterner SM, Bodnar BJ (1984) Synthetic fluid inclusions in natural quartz I. Compositional types synthesised and applications to experimental geochemistry. Geochim Cosmochim Acta 48: 2659–2668

Sushchevskaya TM, Borisov MV (1992) Fluid–rock interaction and cassiterite deposition. In: Water–rock interaction. Balkema, Rotterdam, pp 1625–1627

Suzouki T, Epstein S (1976) Hydrogen isotope fractionations between OH-bearing minerals and water. Geochim Cosmochim Acta 40:1229–1240

Swart R (1987) The Brandberg West formation. A late proterozoic carbonate turbidite? Commun Geol Surv Namib 3:19–23

Taylor HP (1977) Water/rock interactions and the origin of H_2O in granitic batholiths. J Geol Soc (Lond) 133:509–558

Taylor HP Jr, Sheppard SMF (1986) Igneous rocks: I. Processes of isotopic fractionation and isotope systematics. In: Valley JW, Taylor HP Jr, O'Niel JR (eds) Stable isotopes in high-temperature geological processes. Reviews in Mineralogy, vol. 16, Mineralogical Society of America, Washington, DC, pp. 227–271

Townshend M (1985) Some aspects of the geology of the vein systems at the Brandberg West mine, South West Africa/Namibia. Thesis, Rhodes University, Grahamstown

van den Kerkhof AM (1990) Isochoric phase diagrams in the systems CO_2–CH_4 and CO_2–N_2: application to fluid inclusions. Geochim Cosmochim Acta 54:621–629

Vennemann TW, O'Neil JR (1993) A simple and inexpensive method of hydrogen isotope and water analyses of minerals and rocks based on zinc reagent. Chem Geol Isot Geosci Sect 103:227–234

Vennemann TW, Smith SMF (1990) The rate and temperature of reaction of ClF_3 with silicate minerals, and their revelance to oxygen isotope analysis. Chem Geol Isot Geosci Sect 86:83–88

Vickers PDF (1984) Comments and recommendations on the SWA tin exploration program. Gold Fields Namibia internal report

Wagener GF (1989) Systematic variation in the tin content of pegmatites in western central Namibia. J Geochem Explor 34:1–19

Walraven FC (1988) Geology and alteration–mineralization in the Gamigab area, north of the Brandberg. Commun Geol Surv Namib 4:83–88

Walraven FC (1989) Geology and alteration–mineralization of the Gamigab tin prospect, Damaraland, Namibia. Dissertation, Rhodes University, p 146

Zheng YF (1991) Calculation of oxygen isotope fractionation in metal oxides. Geochim Cosmochim Acta 57:2299–2307

Zheng YF (1992) Oxygen isotope fractionation in wolframite. Eur J Mineral 4:1331–1335